

---

# PACING OPINION POLARIZATION VIA GRAPH REINFORCEMENT LEARNING \*

---

Mingkai Liao  
 CSSE, Shenzhen University  
 Shenzhen, China  
 {13542830854@163.com}

## ABSTRACT

Opinion polarization moderation has been studied predominantly as an *analytical optimization* problem under the Friedkin–Johnsen (FJ) model, where intervention algorithms are tightly coupled to linear steady-state analysis and model-specific derivations. While effective in narrowly structured settings, such methods scale poorly and do not naturally extend to richer intervention regimes. This raises a central question: can polarization moderation be treated not merely as an analytical domain, but as a *graph-based sequential planning* problem?

We answer this question by proposing **PACIFIER**, to our knowledge the **first unified graph-learning framework**, and in particular the **first graph reinforcement learning framework**, for opinion polarization moderation. PACIFIER reformulates the canonical MODERATEINTERNAL (MI) and MODERATEEXPRESSED (ME) problems as sequential decision-making tasks on graphs, replacing repeated analytical recomputation with learned intervention policies. The framework is instantiated with two complementary variants: **PACIFIER-RL**, which learns long-horizon intervention policies through reinforcement learning, and **PACIFIER-Greedy**, which learns efficient myopic action ranking. Within the same architecture, PACIFIER extends naturally beyond the canonical setting to cost-aware moderation, continuous-valued internal opinions, and topology-altering node removal.

To address the distinctive challenges of topology-preserving moderation, we introduce a temporal-aware node marking mechanism that makes intervention history explicit to the encoder, together with polarization-aware global features that summarize opinion–structure interaction patterns. These components provide a more history-aware and value-relevant state representation while avoiding expensive steady-state recomputation during planning. Under an inductive learning paradigm, PACIFIER is trained only on small synthetic two-echo-chamber graphs with fewer than 50 nodes, yet generalizes effectively to real-world Twitter follow and retweet networks with up to 155,599 nodes.

Experiments on 15 real-world polarized networks reveal a clear regime-dependent picture. In analytically structured MI settings, PACIFIER remains competitive with strong analytical solvers and consistently emerges as the strongest scalable non-analytical alternative. In contrast, in ME, continuous-ME, and cost-ME, PACIFIER achieves strong and highly consistent superiority over non-PACIFIER baselines. Most importantly, **PACIFIER-RL** becomes decisively superior when long-horizon planning truly matters, most notably in cost-ME and topology-altering *node\_removal*, where reasoning over future structural consequences is crucial.

Overall, PACIFIER shifts opinion polarization moderation from a domain dominated by model-specific analytical optimization toward a unified graph-learning and graph-reinforcement-learning paradigm.

**Keywords** Opinion Polarization · Graph Reinforcement Learning · Network Intervention · Opinion Dynamics · Social Networks

---

\**Citation:* Authors. Title. Pages.... DOI:000000/11111.

## 1 Introduction

Opinion polarization has emerged as one of the most pressing challenges in contemporary online social networks, with far-reaching consequences for democratic discourse, public health, and societal stability. Extensive empirical evidence documents the formation of “echo chambers” and “filter bubbles,” in which individuals become increasingly insulated within homogeneous information environments that reinforce pre-existing beliefs while marginalizing opposing viewpoints. Such polarization is not merely a theoretical concern; it has been linked to political fragmentation, large-scale misinformation diffusion, and adverse public health outcomes during societal crises. Addressing opinion polarization therefore calls for principled, scalable, and adaptable computational intervention frameworks capable of operating on large and heterogeneous social networks.

A foundational line of work on algorithmic polarization moderation was established by Matakos et al. [1], who formalized two canonical intervention problems under the Friedkin–Johnsen (FJ) opinion dynamics model [2]: `MODERATEINTERNAL` (MI) and `MODERATEEXPRESSED` (ME). These problems capture two complementary intervention paradigms: modifying individuals’ internal (stubborn) opinions and directly regulating their expressed opinions. Leveraging the linear-algebraic structure of the FJ model, prior work proposed efficient heuristics such as Binary Orthogonal Matching Pursuit (BOMP) for MI and greedy selection strategies for ME. While analytically elegant and effective in strictly linear settings, these approaches are tightly coupled to model-specific assumptions and steady-state closed-form analysis. Consequently, they are difficult to generalize to cost-aware interventions, nonlinear opinion dynamics, or topology-altering mechanisms such as node removal.

More broadly, polarization moderation is computationally challenging and often NP-hard [3], limiting the scalability of classical optimization-based approaches. Even polynomial-time methods such as BOMP incur  $O(n^2)$  complexity, which becomes prohibitive on large real-world graphs. Moreover, once nonlinear opinion dynamics or heterogeneous intervention constraints are introduced, steady-state closed-form analysis may no longer exist or may become analytically intractable. These limitations motivate the search for a unified framework that (i) scales to large networks, (ii) adapts across intervention paradigms, and (iii) remains robust under structurally consistent nonlinear extensions of the FJ model.

**The primary contribution of this work** is the introduction of **PACIFIER**, a graph reinforcement learning framework for sequential polarization moderation. We reformulate the MI and ME problems as sequential decision-making tasks over networked opinion dynamics, enabling the learning of adaptive intervention policies without relying on repeated steady-state recomputation or handcrafted heuristics. Unlike prior analytical approaches, PACIFIER is objective-agnostic: the agent optimizes any polarization-related objective specified through its reward function. Within this unified paradigm, we demonstrate that PACIFIER naturally extends beyond the original linear MI/ME settings to several practically relevant regimes, including cost-aware intervention, continuous-valued internal opinions, and topology-altering node removal.

Empirically, PACIFIER exhibits strong and consistent performance across diverse tasks and datasets. On 15 real-world Twitter follow and retweet networks (up to 155,599 nodes), PACIFIER-RL achieves a 100% win rate over the strongest non-learning baselines in expressive-opinion moderation (ME and ME-cost), yielding substantial reductions in accumulated polarization. Under cost-aware MI settings, both the RL and greedy variants consistently outperform all classical baselines. Even in nonlinear and topology-changing regimes—where traditional analytical methods lose their structural advantages—PACIFIER-RL maintains robust superiority. At the same time, in strictly linear MI settings where near-optimal analytical solvers exist, PACIFIER remains competitive, demonstrating that learning-based policies do not sacrifice performance in regimes where closed-form solutions are strong.

Inspired by the success of graph reinforcement learning in network intervention problems such as network dismantling [4], PACIFIER bridges structural graph optimization and opinion dynamics by jointly modeling network topology, opinion evolution, and intervention history. Adopting an inductive training paradigm, the agent is trained on small synthetic graphs and directly generalizes to large-scale real networks, enabling scalable deployment across heterogeneous social systems.

**Our second major contribution** addresses two representation challenges unique to polarization moderation under topology-preserving interventions.

First, when the network structure  $G = (V, E)$  remains fixed and interventions only modify node or edge attributes, different intervention histories may produce nearly indistinguishable graph observations. This history-induced ambiguity leads to state aliasing and unstable credit assignment in graph reinforcement learning. We formalize topology-preserving interventions in Definition 3.2 and introduce a temporal-aware node marking mechanism that explicitly encodes intervention history into node features, ensuring that the encoder distinguishes otherwise identical states.

Second, we incorporate polarization-aware global signals into the state encoder by combining node-level opinion features with graph-level structural cues. These features correlate with polarization regimes and guide value estimation without requiring expensive steady-state recomputation during planning.

Together, these representation mechanisms enable PACIFIER to operate effectively across topology-preserving and topology-altering regimes, establishing it as a unified, scalable, and extensible framework for moderating opinion polarization under diverse dynamical and intervention settings.

## 1.1 Contributions

The main contributions of this work are summarized as follows:

- **PACIFIER: a unified graph reinforcement learning framework for polarization moderation.** We propose **PACIFIER**, a graph reinforcement learning framework that reformulates the canonical **MODERATEINTERNAL** (MI) and **MODERATEEXPRESSED** (ME) problems as sequential decision-making tasks over networked opinion dynamics. Unlike prior analytical or heuristic methods tied to steady-state closed-form analysis, **PACIFIER** learns adaptive intervention policies directly through interaction, enabling scalable optimization on large social networks without repeated recomputation of equilibrium solutions.
- **Generalization across intervention paradigms and FJ-consistent dynamics.** Within a single objective-agnostic learning framework, **PACIFIER** extends beyond the original linear MI/ME settings to multiple practically relevant regimes, including cost-aware interventions, continuous-valued internal opinions, and topology-altering node removal. This establishes a unified moderation paradigm that remains robust under structurally consistent extensions of the Friedkin–Johnsen model.
- **Representation mechanisms for topology-preserving and polarization-aware learning.** We address two key challenges in graph reinforcement learning for polarization moderation: (i) a temporal-aware node marking mechanism that resolves history-induced state aliasing under topology-preserving interventions, and (ii) polarization-aware global feature integration that improves value estimation without requiring expensive steady-state recomputation. These mechanisms enable stable credit assignment and effective policy learning across diverse intervention regimes.
- **Extensive empirical validation on large-scale real networks.** We evaluate **PACIFIER** on 15 real-world Twitter follow and retweet networks with sizes up to 155,599 nodes across multiple intervention tasks and dynamical regimes. **PACIFIER-RL** achieves a 100% win rate over the strongest non-learning baselines in expressive-opinion moderation (ME and ME-cost), yields nearly 40% average improvement in cost-aware MI settings, and maintains strong superiority under nonlinear and topology-changing interventions. At the same time, **PACIFIER** remains competitive with near-optimal analytical solvers in strictly linear MI settings, demonstrating both robustness and adaptability across regimes.

## 1.2 Paper Organization

The remainder of this paper is organized as follows. Section 2 reviews related work on opinion polarization, moderation algorithms, and graph reinforcement learning. Section 3 formalizes the **MODERATEINTERNAL** and **MODERATEEXPRESSED** problems under the Friedkin–Johnsen model and introduces FJ-consistent nonlinear and extended intervention settings. Section 4 presents the **PACIFIER** framework, including the reinforcement learning formulation, the temporal-aware node marking mechanism, and the polarization-aware feature design. Section 5 reports experimental results on synthetic and real-world networks across base and extended regimes. Finally, Section 6 concludes the paper and discusses future research directions.

## 2 Related Work

Despite substantial progress in both opinion-dynamics modeling and network intervention, existing approaches remain divided between model-specific analytical optimization and learning-based structural intervention, with limited integration across the two paradigms. Our work lies at the intersection of three research directions: (i) opinion polarization modeling and algorithmic moderation under opinion dynamics, (ii) traditional network intervention and key-player identification, and (iii) graph reinforcement learning for sequential decision making on networks. We briefly review each stream and clarify how **PACIFIER** bridges the gap between analytical polarization moderation and modern learning-based network intervention.

## 2.1 Opinion Polarization and Moderation

**Opinion polarization.** Opinion polarization in online social systems is commonly studied through social influence and opinion formation models. A foundational computational framework is the Friedkin–Johnsen (FJ) model [2], where each user maintains a persistent *internal* opinion and iteratively forms an *expressed* opinion as a weighted average of her own internal belief and her neighbors’ expressed opinions. Under mild conditions, the system converges to a unique steady state. Building on this model, Matakos et al. [1] introduced a principled *polarization index* defined on the steady-state expressed opinion vector,  $\pi(z) = \|z\|_2^2/n$ , and provided an interpretation via absorbing random walks and the influence operator  $Q = (L + I)^{-1}$  mapping internal to expressed opinions ( $z = Qs$ ). This formulation captures the echo-chamber phenomenon: polarization becomes high when graph communities align with homogeneous extreme internal opinions, and remains low when opinions are well-mixed across communities.

**The MI/ME moderation problems.** Within this framework, Matakos et al. [1] formalized two canonical moderation problems. In MODERATEINTERNAL (MI), a budgeted subset of users is selected and their internal opinions are neutralized to minimize  $\pi(z)$ . In MODERATEEXPRESSED (ME), a budgeted subset of users is selected and their expressed opinions are directly fixed to neutral. Both problems are NP-hard and the objective is non-monotone in the selected set, making naive greedy reasoning unreliable [1]. These formulations have become the standard benchmarks for direct opinion moderation within the FJ paradigm.

**Algorithms and limitations under the FJ model.** To solve MI and ME, Matakos et al. [1] proposed model-aware heuristics that exploit the linear-algebraic structure of the FJ steady state. For MI, Binary Orthogonal Matching Pursuit (BOMP) leverages the global influence operator to guide node selection and can achieve strong performance in strictly linear settings. However, this global reasoning induces scalability challenges: selection requires manipulating dense influence information, yielding complexity on the order of  $O(kn^2)$ , which becomes prohibitive for large networks. For ME, greedy-style strategies and lightweight heuristics such as *ExtremeExpressed* and *ExtremeNeighbors* were proposed. These approaches typically require recomputing or approximating steady-state opinions after each intervention step in order to rescore candidates, introducing substantial per-step overhead.

More importantly, these algorithms critically depend on linear steady-state analysis. Once cost-aware constraints, nonlinear opinion dynamics, or topology-altering interventions are introduced, closed-form influence operators may no longer exist or may become analytically intractable. This limits the direct applicability of model-specific heuristics beyond the original linear FJ setting.

**Depolarization via exposure and topology modification.** Beyond direct opinion moderation, related work has explored reshaping exposure patterns or network topology to reduce polarization. Representative approaches include adding cross-cutting edges [5, 6], optimizing edge additions under disagreement objectives [7], and studying adversarial or strategic behaviors within FJ-style dynamics [8]. Recent learning-based approaches also model depolarization as a sequential decision problem and learn policies from simulated interactions [9]. These works highlight the diversity of intervention primitives but do not provide a unified framework that scales across MI/ME-style direct moderation and FJ-consistent extensions.

## 2.2 Traditional Network Intervention Algorithms

The broader problem of identifying influential or critical nodes has been extensively studied in network science under tasks such as key-player identification, critical node detection, and network dismantling. The critical node problem aims to remove a limited number of nodes to maximally disrupt connectivity, with early formulations developed in operations research [10]. Subsequent work proposed scalable dismantling strategies motivated by percolation and robustness analysis [11].

Traditional intervention algorithms generally fall into several categories:

- **Greedy approaches**, which iteratively select nodes based on immediate objective improvement;
- **Spectral and relaxation methods**, leveraging eigen-structure of graph matrices;
- **Message-passing techniques**, exploiting approximate local factorization;
- **Combinatorial optimization**, including integer programming formulations.

While powerful for purely structural objectives such as connectivity or fragmentation, these methods typically do not incorporate evolving dynamical state variables such as opinions, nor do they model history-dependent intervention effects. In polarization moderation, the objective depends on the steady state of an opinion dynamics process, and the

most influential nodes are not necessarily those that maximize structural centrality or connectivity disruption. This mismatch motivates learning-based planners capable of jointly reasoning about structure, dynamics, and intervention history.

### 2.3 Graph Reinforcement Learning on Networks

Recent advances in deep reinforcement learning (DRL) have enabled learning-based solutions to combinatorial optimization on graphs, particularly for sequential decision problems where myopic greedy choices can be suboptimal. A representative breakthrough is FINDER [4], which formulates network dismantling as a Markov decision process and learns removal policies using deep Q-learning with graph neural encoders. FINDER demonstrated that an agent trained on small synthetic graphs can generalize to much larger real networks, achieving strong empirical scalability.

However, most graph-RL frameworks focus on *structural* objectives under *topology-altering* interventions. In contrast, opinion moderation tasks involve *dynamical state evolution* and may be *topology-preserving*: the underlying graph often remains invariant while only node attributes (internal or expressed opinions) and intervention history change. This creates unique representation challenges. When topology is fixed, distinct intervention histories may yield graph observations that appear identical if history is not explicitly encoded, resulting in state aliasing and unstable value estimation. Furthermore, when opinions are continuous-valued or governed by nonlinear but topology-preserving dynamics, structural encoders alone may be insufficient to capture polarization-relevant signals.

### 2.4 Research Gap and Our Contribution

Despite advances in polarization moderation and graph reinforcement learning, a methodological gap remains. Model-specific analytical approaches provide strong guarantees in strictly linear settings but lack flexibility and scalability under cost-aware, nonlinear, or topology-changing regimes. Conversely, graph-RL methods offer scalable inductive learning paradigms but have largely focused on structural objectives rather than dynamical polarization minimization.

PACIFIER bridges this gap by formulating MODERATEINTERNAL and MODERATEEXPRESSED—and their FJ-consistent extensions—as sequential decision problems over networked opinion dynamics. Our framework is objective-agnostic and accommodates multiple intervention paradigms, including cost-aware moderation, and node removal, while preserving the underlying influence topology when appropriate. To address topology-preserving aliasing, we introduce a temporal-aware node marking mechanism, and to enhance value estimation, we incorporate polarization-aware global features.

Empirically, this unified graph-RL formulation not only remains competitive with near-optimal analytical solvers in strictly linear MI settings, but also substantially outperforms classical baselines in cost-aware, nonlinear, and topology-altering regimes, where steady-state-based heuristics lose structural advantages. This establishes a scalable and extensible learning-based paradigm for opinion polarization moderation.

## 3 Problem Formulation: MI/ME Moderation under the Friedkin–Johnsen Paradigm: One-Shot Planning and ANP Evaluation

This section formally defines the opinion polarization moderation problems studied in this work. We begin by reviewing the Friedkin–Johnsen (FJ) opinion dynamics model and the associated polarization index. We then define the MODERATEINTERNAL and MODERATEEXPRESSED problems under this model. Finally, we introduce our *one-shot planning constraint*—which requires committing to a complete intervention sequence using only the initial instance information—and the *accumulated normalized polarization (ANP)* evaluation metric that measures the area-under-curve of polarization along the intervention trajectory, together characterizing the setting targeted by our PACIFIER framework.

### 3.1 Friedkin-Johnsen Opinion Dynamics Model

We consider a social network represented as an undirected, weighted graph  $G = (V, E)$ , where  $|V| = n$  denotes the set of individuals and  $E$  represents the social ties between them. Each edge  $(i, j) \in E$  is associated with a weight  $w_{ij} \geq 0$ , signifying the strength of influence between individuals  $i$  and  $j$ . Each individual  $i \in V$  also has a *self-weight*  $w_{ii} > 0$ , which quantifies their level of attachment to their own internal belief.

The opinion formation process is governed by the Friedkin–Johnsen (FJ) model [2]. In this model, each individual  $i$  maintains two types of opinions:

- **Internal opinion** ( $s_i$ ): a persistent belief, represented as a scalar value. In our setting,  $s_i \in [-1, 1]$ , where  $-1$  and  $1$  represent two opposing extreme stances, and  $0$  represents a neutral stance.
- **Expressed opinion** ( $z_i$ ): a publicly stated opinion that evolves over time based on social influence.

The update rule for the expressed opinion of individual  $i$  is a weighted average of their own internal opinion and the current expressed opinions of their neighbors:

$$z_i = \frac{w_{ii}s_i + \sum_{j \in N(i)} w_{ij}z_j}{w_{ii} + \sum_{j \in N(i)} w_{ij}}, \quad (1)$$

where  $N(i)$  denotes the set of neighbors of node  $i$  in  $G$ . It is well-established that this iterative process converges to a unique *steady-state* expressed opinion vector  $\mathbf{z}$  for any initial condition.

The steady-state vector  $\mathbf{z}$  can be computed directly in closed form using the network structure and the internal opinion vector  $\mathbf{s}$ . Let  $L$  be the Laplacian matrix of graph  $G$ . The fundamental matrix  $Q$  is defined as:

$$Q = (L + I)^{-1}. \quad (2)$$

The steady-state expressed opinions are then given by:

$$\mathbf{z} = Q\mathbf{s}. \quad (3)$$

### 3.2 Polarization Index

Following [1], we quantify the level of polarization in the network using the *polarization index* based on the steady-state expressed opinion vector.

**Definition 3.1** (Polarization Index). Given a network  $G = (V, E)$ , a vector of internal opinions  $\mathbf{s}$ , and the resulting steady-state vector of expressed opinions  $\mathbf{z}$ , the polarization index  $\pi(\mathbf{z})$  is defined as:

$$\pi(\mathbf{z}) = \frac{\|\mathbf{z}\|^2}{n}. \quad (4)$$

This quantity is already normalized by the number of nodes  $n$ , so that polarization values are comparable across graphs of different sizes.

### 3.3 Topology-Preserving Interventions

Before introducing the canonical MI and ME problems, we formalize the class of interventions to which they belong.

**Definition 3.2** (Topology-preserving intervention). An intervention process is *topology-preserving* if, throughout the decision horizon, the graph topology remains exactly unchanged: no nodes or edges are removed, added, rewired, or reweighted. Formally, the graph structure  $G = (V, E)$  is invariant over time, and interventions modify only node- or edge-level *attributes* (e.g., internal opinions, expressed opinions, or fixed-value boundary conditions), while keeping the adjacency structure fixed.

In topology-preserving settings, the observable graph connectivity does not directly reveal which nodes have been intervened on. Consequently, two intervention histories that differ in selected nodes may induce identical or nearly identical adjacency structures. This creates a representation ambiguity under permutation-invariant message-passing encoders, where structurally identical graphs with different intervention histories can produce indistinguishable aggregated embeddings.

Such ambiguity leads to a fundamental challenge:

- **History-induced state aliasing:** different intervention trajectories may correspond to states that are structurally identical but behaviorally distinct.

The MI and ME problems defined below are canonical examples of topology-preserving moderation, as they modify internal or expressed opinions without altering the underlying network structure.

### 3.4 Canonical Moderation under One-Shot Planning with ANP Evaluation

We now formalize the two key intervention problems for reducing polarization and integrate them with the planning constraint and evaluation criterion that define the final setting studied in this work.

Throughout, we assume a budget  $k$ , and the goal is to select  $k$  individuals to *moderate*, i.e., to set the targeted opinion attribute to a neutral state ( $0$ ), such that the resulting polarization index is minimized.

### 3.4.1 The MODERATEINTERNAL Problem

**Problem 3.1** (MODERATEINTERNAL). Given a graph  $G = (V, E)$ , an internal opinion vector  $\mathbf{s} \in [-1, 1]^n$  (binary in the base setting, continuous in our extension), and an integer budget  $k > 0$ , find a set  $T_s \subset V$  with  $|T_s| = k$  such that the polarization index is minimized after setting  $s_i = 0$  for all  $i \in T_s$ . Let  $\mathbf{s}'$  denote the modified internal opinion vector, and let  $\mathbf{z}'$  be the resulting steady-state expressed opinion vector under the FJ model (i.e.,  $\mathbf{z}' = Q\mathbf{s}'$  in the linear case). The objective is:

$$\min_{T_s \subset V, |T_s|=k} \pi(\mathbf{z}') = \frac{1}{n} \|Q\mathbf{s}'\|^2.$$

### 3.4.2 The MODERATEEXPRESSED Problem

**Problem 3.2** (MODERATEEXPRESSED). Given a graph  $G = (V, E)$ , an internal opinion vector  $\mathbf{s}$  (binary in the base setting, continuous in our extension), the corresponding steady-state expressed opinion vector  $\mathbf{z}$ , and an integer budget  $k > 0$ , find a set  $T_z \subset V$  with  $|T_z| = k$  such that the polarization index is minimized after fixing  $z_i = 0$  for all  $i \in T_z$ . The dynamics are recalculated under this constraint, leading to a new steady-state vector  $\mathbf{z}'$ . The objective is:

$$\min_{T_z \subset V, |T_z|=k} \pi(\mathbf{z}') = \frac{1}{n} \|\mathbf{z}'\|^2.$$

While the MI and ME problems above specify *what* is being intervened on, they do not specify *how* intervention sequences are constructed nor *how* they are evaluated over time. We now integrate them with the planning and evaluation regime that defines the final decision problem studied in this work.

**One-shot planning constraint (plan once from the initial instance).** Let  $\mathbf{z}^{(0)}$  denote the converged expressed-opinion vector (i.e., the FJ *settled opinions*) under the original instance, so  $\mathbf{z}^{(0)} = \mathbf{z}$  in (3). The planner observes only the *initial* instance information

$$\mathcal{I}_0 = (G, \mathbf{s}, \mathbf{z}^{(0)}, k) \quad (\text{and costs if applicable}),$$

and must output a complete ordered intervention sequence

$$(v_1, \dots, v_k)$$

*in a single planning pass.*

Crucially, executing an action changes the opinion system. For MI, intervening on  $v_t$  modifies the internal opinion (stubbornness anchor) of that node, e.g.,  $s(v_t) \leftarrow 0$ ; for ME, intervening on  $v_t$  fixes the expressed opinion of that node, e.g.,  $z(v_t) \leftarrow 0$ , which acts as an exogenous constraint in the subsequent opinion-formation process. If one were to execute the first  $t$  actions and then re-run the opinion dynamics to convergence, one would obtain a new limiting vector of settled opinions, denoted by  $\mathbf{z}^{(t)}$ .

Under the one-shot constraint, such intermediate settled-opinion states are *not available* to the planner during selection: the algorithm is **not allowed** to recompute, query, or otherwise use any  $\mathbf{z}^{(t)}$  induced by partial prefixes  $\{v_1, \dots, v_t\}$ . Equivalently, the planned sequence must be a function of  $\mathcal{I}_0$  alone,

$$(v_1, \dots, v_k) = \Pi(\mathcal{I}_0).$$

**Why one-shot planning?** A key property of MI/ME-style moderation is that it is *topology-preserving*: the social graph is treated as fixed, and interventions act on opinion-related attributes (internal or expressed) rather than rewiring links. At the same time, polarization is tightly coupled with echo-chamber structure—when opposing camps are well-separated by the topology, the steady-state opinions tend to become more extreme and more segregated. This coupling makes multi-round “intervene–re-equilibrate–replan” pipelines problematic in two ways. First, they are computationally expensive because each additional round requires re-solving (or simulating) the opinion dynamics to a settled state, which becomes a major bottleneck on large graphs and can be infeasible under nonlinear or non-analytic dynamics. Second, repeated replanning is methodologically misaligned with deployment: it implicitly assumes the influence topology remains stable long enough for opinions to settle after every partial intervention, whereas real platforms may exhibit structural drift or co-evolution over the same horizon, undermining the validity of repeatedly conditioning on intermediate equilibria. These considerations motivate a *plan-once* regime: the planner commits to a complete ordered intervention sequence using only the initial instance information, while intermediate settled-opinion states are computed *only* for evaluation.

**What this rules out.** This explicitly excludes “select-and-recompute” heuristics for MI/ME that repeatedly: (a) apply one intervention, (b) re-equilibrate the dynamics to obtain the new settled opinions, and then (c) use the updated settled-opinion state to score and select the next node.

**Accumulated normalized polarization (ANP).** Although planning is restricted as above, we evaluate a produced sequence  $(v_1, \dots, v_k)$  using an accumulated score that rewards *earlier* and *more consistent* polarization reduction along the trajectory. Let  $\mathbf{z}^{(t)}$  denote the converged expressed-opinion vector (the settled opinions) *for evaluation purposes* after applying the first  $t$  interventions in the sequence, for  $t = 0, 1, \dots, k$ .

We view the budget horizon as a normalized progress axis:

$$x_t = \frac{t}{k} \in [0, 1],$$

so the full sequence  $(v_1, \dots, v_k)$  traces a polarization trajectory from  $x_0 = 0$  (no intervention) to  $x_k = 1$  (all  $k$  interventions executed).

Recall that the polarization index  $\pi(\mathbf{z}) = \|\mathbf{z}\|_2^2/n$  is already normalized by the graph size  $n$ . Following the trajectory-level normalization idea used in accumulated normalized connectivity (ANC) [4], we further define the stepwise normalized polarization score as

$$\tilde{\pi}(\mathbf{z}^{(t)}) = \frac{\pi(\mathbf{z}^{(t)})}{n} = \frac{\|\mathbf{z}^{(t)}\|_2^2}{n^2}. \quad (5)$$

We then define the accumulated normalized polarization (ANP) score as

$$\mathcal{R}_{\text{ANP}}(v_1, \dots, v_k) = \frac{1}{k+1} \sum_{t=0}^k \tilde{\pi}(\mathbf{z}^{(t)}). \quad (6)$$

The quantity  $\mathcal{R}_{\text{ANP}}$  can be viewed as a discrete approximation to the area under the polarization trajectory curve over the normalized horizon  $x \in [0, 1]$ . Lower values indicate that polarization is reduced earlier and more persistently throughout the intervention trajectory.

### 3.5 Computational Complexity

Both MI and ME are computationally challenging, as established in [1].

**Theorem 3.1** ([1]). *The MODERATEINTERNAL problem is NP-hard.*

**Theorem 3.2** ([1]). *The MODERATEEXPRESSED problem is NP-hard.*

### 3.6 Extended Tasks Beyond the Canonical FJ Setting

The MI and ME problems defined above correspond to the canonical unweighted setting under the linear Friedkin–Johnsen (FJ) model, with binary internal opinions and topology-preserving interventions. To broaden the moderation problem space while remaining within the same overall framework, we define three extended task families that relax different aspects of this canonical setting. These extensions modify either the opinion representation, the intervention cost structure, or the intervention mechanism, while preserving the objective of minimizing polarization under a fixed budget.

**Extended Task I: Cost-Aware Moderation.** In the canonical MI and ME problems, all interventions are assumed to have equal cost. In this extended task, each node  $v \in V$  is associated with a nonnegative intervention cost  $c(v)$ , representing the relative expense or difficulty of moderating that node.

The planner is still given a budget horizon of  $k$  interventions, but the quality of a solution now depends not only on the achieved polarization reduction, but also on how effectively the intervention sequence uses the available costs over the trajectory. This extension preserves the underlying FJ opinion dynamics and graph topology, but changes the optimization landscape by introducing heterogeneous action costs.

**Extended Task II: Continuous-Opinion Moderation.** In the canonical setting, internal opinions are binary and polarized, i.e.,  $s_i \in \{-1, +1\}$ . In this extended task, internal opinions are allowed to take continuous values in the interval  $[-1, 1]$ .

This extension preserves the same linear FJ opinion dynamics and the same moderation actions as in MI and ME, but relaxes the opinion representation to allow heterogeneous opinion intensities. As a result, users can differ not only in camp membership (negative vs. positive), but also in the strength of their stance. The moderation action still sets the targeted attribute to the neutral value 0, but the resulting intervention problem now depends on a richer continuous opinion landscape.

**Extended Task III: Topology-Altering Moderation (Node Removal).** In the canonical MI and ME problems, interventions are topology-preserving: the graph  $G = (V, E)$  remains unchanged. In this extended task, an intervention removes a selected node from the network.

Formally, selecting a node  $v$  updates the graph as

$$G \leftarrow G \setminus \{v\},$$

removing  $v$  and all its incident edges. Opinion dynamics are subsequently computed on the modified topology.

Unlike MI and ME, this task alters the graph structure itself and therefore changes the influence propagation pattern after each action. The objective remains minimizing polarization under a budget of  $k$  interventions, but the feasible action space now includes structural modification of the network.

**Unified Problem View.** Under all three extended task families, the core objective remains the same: given a graph, an opinion state, and a budget of  $k$  interventions, select an ordered intervention sequence that minimizes polarization.

What changes across tasks is the transition structure of the environment. In cost-aware moderation, the intervention dynamics are unchanged but actions carry heterogeneous costs. In continuous-opinion moderation, the underlying FJ dynamics remain linear, but the opinion space becomes richer by allowing heterogeneous opinion magnitudes. In topology-altering node removal, each action changes the graph itself, modifying future influence propagation and making long-horizon structural effects central to the decision process.

Together, these tasks define an expanded moderation problem space that extends the canonical MI/ME formulation along three complementary dimensions: cost structure, opinion representation, and intervention mechanism. This provides a broader testbed for evaluating whether a moderation framework can generalize beyond the original binary, unweighted, topology-preserving setting while preserving the same overall goal of polarization reduction.

## 4 PACIFIER Framework

PACIFIER is a graph-based learning framework for *sequential* polarization moderation on networks. It is designed to (i) learn intervention policies from simulated graph–opinion interactions and (ii) deploy them efficiently on large real-world graphs via lightweight feed-forward inference. PACIFIER follows a two-phase workflow: (i) *offline training* on a distribution of synthetic graph–opinion instances, and (ii) *deployment-time application* on a target network without iterative recomputation during planning.

PACIFIER supports two closely related variants within the same architecture: **PACIFIER-RL**, which learns a long-horizon intervention policy via bootstrapped value-based reinforcement learning, and **PACIFIER-Greedy**, a myopic variant that learns to approximate *immediate* polarization reduction without bootstrapping. Both variants share the same encoder–decoder representation and differ only in their learning objectives and exploration strategies (Sec. 4.4).

**Overview and components.** Moderation under MI/ME-type interventions typically differs from topology-altering structural control: in many practical settings the graph topology remains fixed, while polarization evolves through opinion dynamics and the *history of past interventions*. This setting motivates PACIFIER’s design around three core components, each addressing a distinct bottleneck for scalable sequential decision making.

**Two-echo-chamber training instances (structured initialization).** Sequential policies require diverse training trajectories, yet purely random graphs and opinion assignments often fail to expose meaningful polarized regimes. PACIFIER therefore trains on a structured distribution of synthetic instances with two opposing communities (echo chambers) and aligned initial opinions (Sec. 4.1). By controlling cross-group exposure (inter-group edge ratio), we generate a spectrum of polarization regimes, which improves robustness and inductive generalization from small training graphs to large test graphs.

**Encoder (history-aware and polarization-aware state representation).** In topology-preserving moderation, the adjacency alone cannot reveal which nodes have been intervened on. Consequently, distinct intervention histories can appear nearly identical to permutation-invariant message-passing encoders, leading to *history-induced state aliasing* and unstable value learning. PACIFIER’s encoder explicitly encodes intervention history through temporal-aware node marking, and augments learned embeddings with polarization-related auxiliary features that summarize opinion–structure interaction patterns (Sec. 4.2). This provides value-relevant global signals without requiring repeated steady-state recomputation as part of the policy input.

**Decoder (parallel action scoring for scalable deployment).** At each step, the decision is to select one feasible node to intervene on. To scale to large graphs, PACIFIER uses a value-based decoder that scores *all* candidate nodes in parallel from shared node/graph embeddings and auxiliary features (Sec. 4.3). A feasibility mask excludes previously intervened nodes, enabling efficient greedy selection at deployment time.

Together, these modules enable PACIFIER to learn intervention strategies offline and execute them online with lightweight feed-forward planning, while remaining compatible with multiple moderation mechanisms and dynamics (Sec. 4.5).

#### 4.1 Two-Echo-Chamber Training Instance Distribution

PACIFIER follows an inductive learning paradigm and is trained offline on a distribution of synthetic graph–opinion instances. The purpose of this distribution is not to exactly replicate any single real-world network, but to expose the agent to a diverse yet structured set of polarized states that capture dominant regimes observed in practice.

**Two-echo-chamber episode initialization.** Each training episode begins by sampling an initial instance

$$(G, \mathbf{s}^{(0)}, \mathbf{c}) \sim \mathcal{D},$$

where  $G = (V, E)$  is a graph,  $\mathbf{s}^{(0)} \in [-1, 1]^n$  is the initial internal-opinion vector, and  $\mathbf{c} \in \mathbb{R}_{\geq 0}^n$  is an optional vector of intervention costs (with  $\mathbf{c} \equiv \mathbf{1}$  in the unweighted setting). The distribution  $\mathcal{D}$  is designed to generate graph–opinion configurations with diverse yet controlled polarization characteristics.

**Graph size and community partition.** To facilitate inductive generalization, training graphs are generated at relatively small scales. For topology-preserving settings (e.g., MI and ME), the total number of nodes is sampled uniformly from the range  $n \in [18, 50]$ . For topology-altering settings such as node removal, we use slightly larger graphs with  $n \in [30, 50]$  to ensure sufficient structural variability after removals. In all cases, the node set  $V$  is partitioned into two disjoint subsets  $V^+$  and  $V^-$  of equal size (or differing by at most one node when  $n$  is odd), representing two opposing echo chambers.

**Graph structure generation.** To generate polarized yet realistic network structures, we construct  $G$  using a two-group generative process based on the Barabási–Albert (BA) preferential-attachment model. On each subset  $V^+$  and  $V^-$ , we independently generate a scale-free subgraph using the BA model, yielding heterogeneous degree distributions within each group.

To control the strength of cross-group exposure, we then add a set of inter-group edges between  $V^+$  and  $V^-$ . The number of such edges is sampled as a fraction of the total number of intra-group edges, and each inter-group edge connects a node chosen uniformly at random from  $V^+$  to one chosen uniformly at random from  $V^-$ . By varying the inter-group edge ratio, this procedure produces graphs ranging from highly segregated (strong polarization) to weakly mixed (low polarization), while preserving scale-free degree characteristics.

**Internal opinion initialization.** Given the generated graph  $G$ , internal opinions are initialized according to the group assignment:

$$s_i^{(0)} = \begin{cases} +1, & i \in V^+, \\ -1, & i \in V^-. \end{cases}$$

This alignment between network communities and opinion camps serves as a canonical polarized starting point. For continuous-opinion settings, this initialization can be extended by sampling opinion magnitudes from bounded continuous distributions with the same sign structure, or by adding controlled noise.

**Intervention cost initialization.** For cost-weighted intervention settings, each node  $i \in V$  is assigned a nonnegative intervention cost  $c_i$ , independently sampled from a fixed distribution. The cost represents the relative difficulty or expense of moderating node  $i$ . In unweighted settings, all nodes are assigned unit cost.

**Empirical motivation from real-world polarized graphs.** To justify the above synthetic training distribution, we analyze the real-world Twitter follow and retweet graphs used in our experiments. For each dataset, nodes are partitioned into two camps according to the sign of their internal-opinion labels, and we compute a set of partition-aware structural statistics.

Across datasets, we observe that these statistics consistently fall within the range spanned by the synthetic BA-based two-group graphs generated by  $\mathcal{D}$ . In particular, real graphs exhibit (i) strong within-camp connectivity, (ii) sparse but

non-negligible cross-camp exposure, and (iii) degree heterogeneity compatible with preferential-attachment structure. These observations indicate that the proposed training distribution captures dominant polarization regimes present in real data, thereby narrowing the train–test distribution gap and improving generalization.

## 4.2 Encoding

The encoding module maps the current moderation state into vector representations that can be reused to score all candidate nodes efficiently. Compared with topology-altering intervention tasks (e.g., node removal), MI/ME-type moderation is typically *topology-preserving*: the underlying graph topology remains unchanged across decision steps, while only node attributes (opinions) and the intervention history evolve over time.

**(Innovation 1) Node Features (Temporal-aware marking).** Let  $S_t \subseteq V$  denote the set of nodes that have already been intervened by step  $t$ . In topology-preserving moderation, the adjacency structure alone does not encode intervention history; consequently, different intervention sequences may produce graph states that are indistinguishable if history is not explicitly represented. To resolve this issue, PACIFIER explicitly encodes intervention history into node features via a temporal-aware marking mechanism. Each node  $v$  is assigned a feature vector

$$\mathbf{x}_t(v) = [s_t(v), s_0(v), \text{mark}_t(v), c(v)], \quad (7)$$

where  $s_t(v)$  is the current opinion attribute after previous interventions,  $s_0(v)$  is the initial opinion attribute at the beginning of the episode,  $\text{mark}_t(v) = \mathbb{I}[v \in S_t]$  indicates whether node  $v$  has already been intervened, and  $c(v) \geq 0$  denotes an optional node-specific intervention cost (set to a constant in unweighted settings). The feasibility mask is consistent with the marking feature:

$$\mathbf{m}_t(v) = 1 - \text{mark}_t(v),$$

so nodes that have already been selected are excluded from future actions.

**(Innovation 2) Polarization-related Auxiliary Features.** PACIFIER augments learned embeddings with a deterministic auxiliary feature vector  $\mathbf{u}_t$  that summarizes intervention progress and opinion–structure interaction patterns. Concretely, let  $n = |V|$  and  $m = |E|$ . We include the covered-node ratio

$$u_t^{(1)} = \frac{|S_t|}{n}. \quad (8)$$

Let  $E_{\text{cov}}(t) = \{(i, j) \in E \mid i \in S_t \text{ or } j \in S_t\}$  denote edges incident to covered nodes. The covered-edge ratio is

$$u_t^{(2)} = \frac{|E_{\text{cov}}(t)|}{m}. \quad (9)$$

To characterize cross-camp interactions among active edges, define

$$E_{\pm}(t) = \{(i, j) \in E \setminus E_{\text{cov}}(t) \mid \text{sign}(s_t(i)) \neq \text{sign}(s_t(j))\},$$

and include

$$u_t^{(3)} = \frac{|E_{\pm}(t)|}{m}. \quad (10)$$

We further include a two-hop structural statistic on the active subgraph  $G[V \setminus S_t]$ . Let  $d_t(v)$  denote the degree of node  $v$  in this subgraph. Define

$$T(t) = \sum_{v \notin S_t} \binom{d_t(v)}{2}, \quad u_t^{(4)} = \frac{T(t)}{n^2}. \quad (11)$$

To further capture sign-based community cohesion, we compute two-hop statistics separately within the positive and negative opinion groups. Define

$$V_t^+ = \{v \notin S_t \mid s_t(v) > 0\}, \quad V_t^- = \{v \notin S_t \mid s_t(v) \leq 0\}.$$

Let  $T^+(t)$  and  $T^-(t)$  denote the corresponding two-hop counts within the induced subgraphs on  $V_t^+$  and  $V_t^-$ . We include

$$u_t^{(5)} = \frac{T^+(t)}{n^2}, \quad u_t^{(6)} = \frac{T^-(t)}{n^2}. \quad (12)$$

The complete auxiliary feature vector is

$$\mathbf{u}_t = [u_t^{(1)}, u_t^{(2)}, u_t^{(3)}, u_t^{(4)}, u_t^{(5)}, u_t^{(6)}]. \quad (13)$$

**Encoding Pipeline Overview.** PACIFIER’s encoder takes as input (i) the fixed adjacency structure of  $G$  and (ii) per-node attributes that evolve with interventions, and produces node embeddings and a graph-level embedding that are reused to score all actions in parallel.

**(1) Inputs.** We represent the graph structure through a (sparse) neighbor-sum operator induced by the adjacency matrix, and represent the evolving moderation status through node features  $X_t$  (defined below). In addition, we maintain a *super-node* (a virtual graph token) that is connected to all nodes by directed edges from nodes to the super-node; its role is to aggregate a graph-level summary at each message-passing iteration.

**(2) Feature-to-embedding projection (node initialization).** Each node feature vector  $\mathbf{x}_t(v)$  is first mapped into a latent embedding via a shared linear projection and nonlinearity:

$$\mathbf{h}_v^{(0)} = \sigma(W_0 \mathbf{x}_t(v)), \quad \mathbf{h}_v^{(0)} \leftarrow \text{norm}(\mathbf{h}_v^{(0)}), \quad (14)$$

where  $\text{norm}(\cdot)$  denotes  $\ell_2$  normalization.

**(3) GraphSAGE message passing (node updates).** For  $k = 1, \dots, K$ , nodes aggregate their neighbors’ embeddings and update their own embeddings in a GraphSAGE-style manner:

$$\mathbf{a}_v^{(k)} = \sum_{u \in \mathcal{N}(v)} \mathbf{h}_u^{(k-1)}, \quad (15)$$

$$\mathbf{h}_v^{(k)} = \sigma \left( W_{\text{sage}} \begin{bmatrix} W_{\text{nbr}} \mathbf{a}_v^{(k)} \\ W_{\text{self}} \mathbf{h}_v^{(k-1)} \end{bmatrix} \right), \quad \mathbf{h}_v^{(k)} \leftarrow \text{norm}(\mathbf{h}_v^{(k)}). \quad (16)$$

**(4) Super-node update (graph-level aggregation at each iteration).** In parallel with node updates, the super-node aggregates current node embeddings by a global sum pooling operator:

$$\mathbf{g}^{(k)} = \sum_{v \in V} \mathbf{h}_v^{(k)}, \quad (17)$$

which provides an iteration-synchronized global summary of the evolving opinion/intervention state.

**(5) Encoder outputs.** After  $K$  iterations, the encoder outputs: (i) node embeddings  $\{\mathbf{h}_v\}_{v \in V}$  with  $\mathbf{h}_v = \mathbf{h}_v^{(K)}$ , and (ii) a graph-level embedding  $\mathbf{g}_t$  (we use  $\mathbf{g}_t = \mathbf{g}^{(K)}$ ), together with (iii) deterministic auxiliary features  $\mathbf{u}_t$  and (iv) a feasibility mask  $\mathbf{m}_t$ . These outputs are shared across all candidate actions and are consumed by the decoding module to compute  $Q(s_t, v)$  for every node  $v$ .

### 4.3 Decoding

The decoding module evaluates each feasible node as a candidate intervention based on the representations produced by the encoding stage. PACIFIER adopts a value-based decoding strategy and learns an action-value function  $\hat{Q}(s_t, v)$  that estimates the long-term return of selecting node  $v$  at state  $s_t$ .

**State-action interaction.** Given the embedding  $\mathbf{h}_v$  of a candidate node  $v$  and the graph-level embedding  $\mathbf{g}_t$ , PACIFIER models their interaction through a bilinear transformation:

$$\mathbf{z}_{t,v} = (\mathbf{h}_v \mathbf{g}_t^\top) \mathbf{w}, \quad (18)$$

where  $\mathbf{w}$  is a learnable projection vector. This interaction captures multiplicative effects between the local representation of the selected node and the global state of the network, allowing the decoder to assess how intervening on  $v$  may influence future polarization dynamics at the graph level.

**Q-value prediction.** The interaction vector  $\mathbf{z}_{t,v}$  is concatenated with the auxiliary feature vector  $\mathbf{u}_t$  and mapped to a scalar action value via a shared nonlinear function:

$$Q(s_t, v) = f_\theta \left( \begin{bmatrix} \mathbf{z}_{t,v} \\ \mathbf{u}_t \end{bmatrix} \right), \quad (19)$$

where  $f_\theta(\cdot)$  denotes a multilayer perceptron with ReLU activations. The same function is applied to all candidate nodes, ensuring parameter sharing and inductive generalization across different graphs and intervention stages.

**Action masking.** To enforce feasibility constraints, nodes that have already been intervened are excluded from selection by applying a large negative bias:

$$Q(s_t, v) \leftarrow Q(s_t, v) + (1 - m_t(v)) \cdot (-M), \quad (20)$$

where  $M$  is a sufficiently large constant. This guarantees that infeasible actions are never chosen during decoding.

**Parallel evaluation.** Because the graph-level embedding  $\mathbf{g}_t$  and the auxiliary vector  $\mathbf{u}_t$  are shared across all candidate nodes, the action-value function  $Q(s_t, v)$  can be evaluated for all nodes in parallel. This design enables efficient inference on large graphs and allows PACIFIER to scale to real-world networks without enumerating actions sequentially.

#### 4.4 Method Procedure

We now describe the *end-to-end* decision-making procedure of PACIFIER, including the MDP formulation, offline training of the two variants, and the deployment-time feed-forward execution on a target network. Crucially, the policy input is always the compact representation  $(G, X_t, \mathbf{u}_t, \mathbf{m}_t)$  produced by the encoder, so deployment-time planning does not require iterative steady-state recomputation.

**MDP formulation.** We model sequential polarization moderation as a Markov Decision Process (MDP) over a graph with evolving node attributes. At each decision step, the agent selects one node to intervene on, observes the resulting state transition, and receives a reward that reflects the evaluated polarization after the intervention. An episode corresponds to a full intervention trajectory of length  $k$  (or until no feasible actions remain).

**State.** At step  $t$ , the state is

$$s_t = (G, X_t, \mathbf{u}_t, \mathbf{m}_t),$$

where  $G = (V, E)$  is the (fixed) network,  $X_t \in \mathbb{R}^{n \times d_x}$  is the node-feature matrix,  $\mathbf{u}_t \in \mathbb{R}^{d_u}$  is a graph-level auxiliary feature vector, and  $\mathbf{m}_t \in \{0, 1\}^n$  is an action-feasibility mask. Let  $S_t \subseteq V$  denote the set of already intervened nodes. Then  $\mathbf{m}_t(v) = 0$  for  $v \in S_t$  and  $\mathbf{m}_t(v) = 1$  otherwise. Under MI/ME-style moderation, the topology of  $G$  remains fixed, and state evolution is driven by opinion updates and intervention history encoded in  $X_t$  (Sec. 4.2).

**Action.** An action selects one feasible node:

$$a_t \in \mathcal{A}_t = \{v \in V \mid \mathbf{m}_t(v) = 1\}.$$

For MI-style intervention, executing  $a_t$  sets  $s_t(a_t) \leftarrow 0$ . Other intervention mechanisms (e.g., fixing expressed opinions or node removal) modify only the environment transition while preserving the decision interface.

**Transition.** After applying the intervention, we update  $S_{t+1} = S_t \cup \{a_t\}$  and the feasibility mask accordingly. For topology-preserving settings,  $G$  remains unchanged. For topology-altering extensions (e.g., node removal),  $G$  is updated.

**Reward (trajectory-aware signal).** Let  $\pi(\mathbf{z}^{(t)})$  denote the polarization index computed from the converged expressed opinions after  $t$  interventions. In cost-weighted settings, each node has cost  $c(v)$  and  $C = \sum_{v \in V} c(v)$ . The step reward is defined as

$$r_t = -\frac{\pi(\mathbf{z}^{(t)})}{C} \cdot c(a_t).$$

For unweighted settings,  $c(v) \equiv 1$ .

**Policy parameterization via encode–decode.** Both PACIFIER-RL and PACIFIER-Greedy share the same architecture. The encoder produces node embeddings  $\{\mathbf{h}_v\}$  and a graph-level embedding  $\mathbf{g}_t$  from  $(G, X_t)$ , together with auxiliary features  $\mathbf{u}_t$  (Sec. 4.2). The decoder maps  $(\mathbf{h}_v, \mathbf{g}_t, \mathbf{u}_t)$  to an action-value estimate  $Q_\theta(s_t, v)$  for each node (Sec. 4.3). Feasibility is enforced via  $\mathbf{m}_t$ .

**Offline training. PACIFIER-RL.** During offline training, PACIFIER-RL interacts with sampled synthetic instances from  $\mathcal{D}$  (Sec. 4.1) to generate trajectories  $\{(s_t, a_t, r_t, s_{t+1})\}$  over a fixed horizon (budget)  $k$  (or until no feasible action remains). At each step, the agent observes the state representation  $(G, X_t, \mathbf{u}_t, \mathbf{m}_t)$  and selects one feasible node via an  $\epsilon$ -greedy strategy: with probability  $1 - \epsilon$  it chooses the feasible node with the largest predicted  $Q_\theta(s_t, v)$ , and otherwise samples a feasible node uniformly at random. The exploration rate  $\epsilon$  is annealed from a high initial value to a small final value over training episodes.

We adopt  $n$ -step Q-learning with experience replay. We store transitions  $(s_t, a_t, R_{t:t+n}, s_{t+n})$  in a replay buffer, where the truncated return is

$$R_{t:t+n} = \sum_{i=0}^{n-1} \gamma^i r_{t+i}.$$

The TD target is computed using a periodically updated target network:

$$y_t = R_{t:t+n} + \gamma^n \max_v Q_{\theta^-}(s_{t+n}, v),$$

where  $\theta^-$  denotes the target-network parameters. The encoder–decoder parameters  $\theta$  are optimized by minimizing the mean-squared TD error:

$$\mathcal{L}_{\text{RL}}(\theta) = \mathbb{E} \left[ (Q_{\theta}(s_t, a_t) - y_t)^2 \right].$$

Mini-batches are sampled uniformly from the replay buffer and parameters are updated using Adam. We employ standard stabilizers for deep Q-learning, including (i) experience replay, (ii) a target network, and (iii)  $n$ -step returns.

For training signal, the environment computes the converged expressed-opinion state after each intervention (under the specified opinion dynamics) and evaluates the polarization index  $\pi(\mathbf{z}^{(t)})$  to produce reward  $r_t$ . Crucially, this converged computation is used *only* inside the environment to generate rewards and learning targets; the policy input remains  $(G, X_t, \mathbf{u}_t, \mathbf{m}_t)$  and thus does not require repeated steady-state recomputation during planning, aligning with our non-iterative planning constraint.

**PACIFIER-Greedy.** The greedy variant removes bootstrapping and multi-step returns and learns only from immediate rewards. We store 1-step tuples  $(s_t, a_t, r_t)$  and set the learning target as

$$y_t = r_t.$$

Parameters are optimized by minimizing

$$\mathcal{L}_{\text{Greedy}}(\theta) = \mathbb{E} \left[ (Q_{\theta}(s_t, a_t) - r_t)^2 \right].$$

During training, PACIFIER-Greedy performs *pure exploration* by sampling actions uniformly at random from feasible nodes, i.e.,  $a_t \sim \text{Unif}(\mathcal{A}_t)$ , without any  $\epsilon$ -greedy scheduling or annealing. Thus, PACIFIER-Greedy learns a myopic value estimator that approximates the immediate polarization-reduction effect of each intervention.

**Online application (deployment).** After offline training, both variants are deployed on a target real-world graph in a purely *feed-forward* manner. At each decision step  $t$ , we construct the current state representation  $(G, X_t, \mathbf{u}_t, \mathbf{m}_t)$  (Sec. 4.2) and evaluate  $Q_{\theta}(s_t, v)$  for all nodes in parallel (Sec. 4.3). Feasibility is enforced by the mask  $\mathbf{m}_t$ : nodes with  $\mathbf{m}_t(v) = 0$  (already intervened) are assigned a large negative value and are never selected. The deployed policy is greedy with respect to  $Q_{\theta}$ :

$$a_t = \arg \max_{v \in V} Q_{\theta}(s_t, v) \quad \text{s.t. } \mathbf{m}_t(v) = 1.$$

This yields an ordered intervention sequence  $(v_1, \dots, v_k)$  and requires no additional optimization at test time. Importantly, online application does *not* require repeated steady-state recomputation during planning: while the environment may compute converged expressed opinions for evaluation, the deployed policy relies only on the learned representations and the intervention history encoded in  $(X_t, \mathbf{u}_t, \mathbf{m}_t)$ .

## 4.5 Flexibility

PACIFIER is designed as a modular graph reinforcement learning framework. Different polarization moderation settings are instantiated by modifying the environment transition and reward definition, while the encoder–decoder architecture and the learning procedure remain unchanged. This separation between *decision-making* and *environment dynamics* allows a single trained agent to be applied across a wide range of intervention paradigms.

In particular, the same framework naturally supports the following dimensions of flexibility:

- **Unweighted vs. cost-weighted interventions.** Heterogeneous intervention costs are incorporated by augmenting node features with a cost attribute and by weighting the stepwise reward accordingly. When costs are uniform, the framework reduces to the unweighted setting without any architectural modification.
- **Discrete vs. continuous internal opinions.** PACIFIER operates on both binary opinion assignments (e.g.,  $\{-1, 1\}$ ) and continuous-valued internal opinions. Continuous settings are handled through the same graph encoder, while hierarchical, dynamics-aware auxiliary features summarize opinion-induced interaction patterns at multiple thresholds. This enables effective value estimation without assuming linearity or closed-form steady-state solutions.

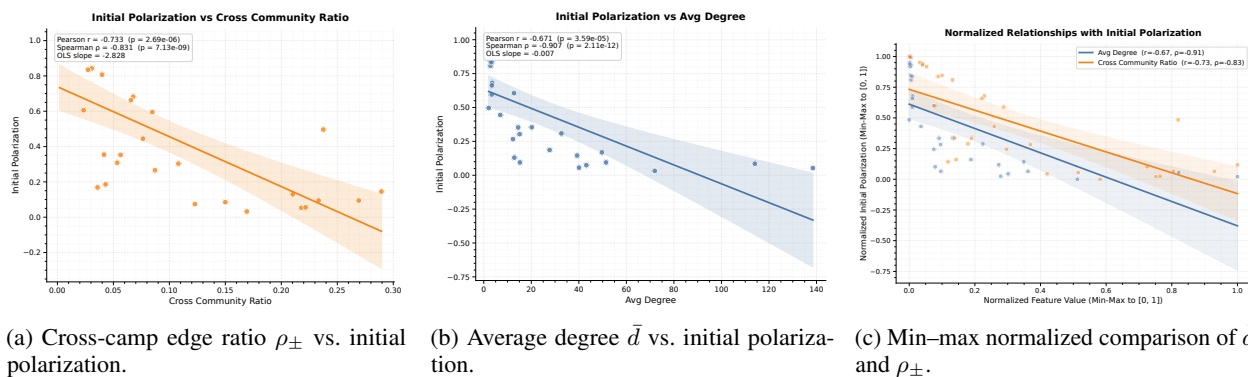


Figure 1: Dataset-level relationships between initial polarization  $\pi(\mathbf{z}^{(0)})$  and two structural indicators across the 31 topic graphs. Higher cross-camp mixing (larger  $\rho_{\pm}$ ) and higher connectivity (larger  $\bar{d}$ ) are associated with lower initial polarization. Pearson and Spearman statistics are reported in the plots.

- **Topology-preserving vs. topology-altering interventions.** Although MI and ME are typically *topology-preserving*, PACIFIER can also accommodate topology-altering interventions such as node removal. In the former case, the graph structure remains invariant and interventions only modify node attributes or impose constraints; in the latter case, the environment transition additionally updates the graph itself. In both settings, the agent continues to operate on the evolving state representation using the same encoder–decoder policy.

Overall, this modularity allows PACIFIER to serve as a unified learning-based intervention framework for a broad class of polarization moderation problems within the Friedkin–Johnsen paradigm, covering binary and continuous opinions, unweighted and cost-weighted interventions, as well as both topology-preserving and topology-altering settings.

## 5 Experiments

In this section, we conduct a comprehensive empirical evaluation of PACIFIER on both synthetic and real-world polarized social networks. Our experiments are designed to answer four questions: (i) how PACIFIER performs against classical baselines on the canonical moderation tasks, (ii) whether the learned policies generalize across graph sizes and from synthetic training graphs to heterogeneous real-world networks, (iii) how PACIFIER behaves in topology-preserving versus topology-altering intervention settings, and (iv) whether the proposed temporal-aware marking and polarization-aware auxiliary features contribute to performance.

To answer these questions, we first describe the datasets, filtering criteria, evaluation protocol, and baselines. We then report results on synthetic benchmarks and real-world datasets, followed by runtime comparisons and an ablation study.

### 5.1 Datasets

All datasets used in our experiments are derived from the benchmark collection introduced by Garimella et al. [12], which provides topic-induced Twitter interaction graphs together with a two-camp partition for each topic. We start from the complete set of topic graphs released in that work and perform a preliminary filtering step to ensure structural validity and consistency for subsequent analysis.

Specifically, we exclude graphs that (i) contain self-loops, or (ii) do not form a single connected component. These conditions are required to guarantee that polarization measures and intervention dynamics are well-defined over the entire graph and are not dominated by isolated nodes or disconnected subgraphs. No filtering is performed based on polarization level or any algorithmic outcome at this stage.

After this structural filtering, we retain 31 topic graphs. For each retained graph, we compute a comprehensive set of structural and polarization-related statistics, including the number of nodes and edges, the sizes of the two camps, the average degree, the initial polarization, the cross-camp edge ratio, as well as the average degrees within each camp. A summary of these statistics is reported in Table 1, which provides an overview of the scale, structural diversity, and polarization characteristics of the datasets used in our experiments.

**Dataset-level correlation analysis.** Beyond the basic statistics in Table 1, we further examine how the initial polarization varies with two intuitive structural indicators across the 31 topic graphs: the average degree  $\bar{d}$  and the

Table 1: Basic statistics of the real-world topic graphs after structural filtering.  $|V|$  and  $|E|$  denote the number of nodes and edges.  $|V^+|$  and  $|V^-|$  denote the sizes of the two opposing camps.  $\bar{d} = 2|E|/|V|$  is the average degree.  $\pi(\mathbf{z}^{(0)})$  is the initial polarization, and  $\rho_{\pm}$  denotes the cross-camp edge ratio.  $\bar{d}^+$  and  $\bar{d}^-$  are the average degrees of nodes in the positive and negative camps, respectively.

Dataset	$ V $	$ E $	$ V^+ $	$ V^- $	$\bar{d}$	$\pi(\mathbf{z}^{(0)})$	$\rho_{\pm}$	$\bar{d}^+$	$\bar{d}^-$
follow_russia_march	1189	16471	612	577	27.706	0.186	0.043	30.828	24.393
follow_baltimore	1441	28291	742	699	39.266	0.145	0.289	57.324	20.097
follow_indiasdaughter	1542	9480	748	794	12.296	0.266	0.087	11.583	12.967
follow_gunsense	1821	103840	884	937	114.047	0.085	0.150	86.482	140.053
follow_germanwings	2111	7329	1087	1024	6.944	0.445	0.076	6.307	7.619
follow_ultralive	2113	16070	1088	1025	15.211	0.095	0.233	19.089	11.094
follow_nemtsov	2156	46529	1046	1110	43.162	0.074	0.123	31.801	53.869
follow_mothersday	2225	14160	1145	1080	12.728	0.606	0.023	13.515	11.894
follow_onedirection	3151	20275	1622	1529	12.869	0.130	0.210	15.482	10.097
follow_ukraine	3383	84035	1642	1741	49.681	0.169	0.036	38.452	60.271
follow_ff	3899	63672	1892	2007	32.661	0.308	0.053	38.958	26.725
follow_nepal	4242	42833	2111	2131	20.195	0.354	0.042	24.500	15.930
follow_netanyahu	4292	297136	2208	2084	138.460	0.053	0.218	197.276	76.145
follow_jurassicworld	4395	31802	2262	2133	14.472	0.353	0.056	13.540	15.460
follow_sxsw	4558	91356	2212	2346	40.086	0.056	0.222	35.411	44.494
follow_beefban	799	6026	411	388	15.084	0.303	0.108	22.470	7.260
follow_indiana	946	24328	459	487	51.433	0.094	0.269	27.941	73.575
follow_leadersdebate	9566	344088	4643	4923	71.940	0.032	0.169	49.798	92.822
retweet_wcw	10674	11809	5379	5295	2.213	0.990	0.002	2.341	2.083
retweet_onedirection	15292	26819	7467	7825	3.508	0.682	0.068	3.224	3.778
retweet_mothersday	155599	176915	77799	77800	2.274	0.943	0.011	2.224	2.324
retweet_russia_march	2134	2951	1089	1045	2.766	0.922	0.014	2.826	2.702
retweet_leadersdebate	25983	44174	12726	13257	3.400	0.663	0.066	3.081	3.707
retweet_jurassicworld	26407	32515	13275	13132	2.463	0.911	0.017	2.601	2.323
retweet_germanwings	29763	39075	15142	14621	2.626	0.843	0.031	2.697	2.552
retweet_nepal	40579	57544	19779	20800	2.836	0.807	0.040	2.389	3.261
retweet_nationalkissingday	4638	4816	2250	2388	2.077	0.496	0.238	1.651	2.478
retweet_ff	5401	7646	2621	2780	2.831	0.984	0.003	2.205	3.422
retweet_gunsense	7106	11483	3647	3459	3.232	0.835	0.027	3.468	2.983
retweet_ultralive	9261	15544	4665	4596	3.357	0.596	0.085	2.760	3.962
retweet_sxsw	9304	11003	4519	4785	2.365	0.930	0.014	2.227	2.496

cross-camp edge ratio  $\rho_{\pm}$ . Figures 1a and 1b show clear negative associations between the initial polarization  $\pi(\mathbf{z}^{(0)})$  and these two indicators. In particular, the relationship between  $\pi(\mathbf{z}^{(0)})$  and the cross-camp edge ratio  $\rho_{\pm}$  is strongly negative (Pearson  $r = -0.733$ ,  $p = 2.69 \times 10^{-6}$ ; Spearman  $\rho = -0.831$ ,  $p = 7.13 \times 10^{-9}$ ), indicating that graphs with stronger cross-camp exposure tend to exhibit substantially lower initial polarization. This observation is consistent with the echo-chamber interpretation of polarization: increasing cross-group connectivity weakens segregation and reduces the extent to which opinions align with community boundaries.

Similarly,  $\pi(\mathbf{z}^{(0)})$  also decreases with the average degree  $\bar{d}$  (Pearson  $r = -0.671$ ,  $p = 3.59 \times 10^{-5}$ ; Spearman  $\rho = -0.907$ ,  $p = 2.11 \times 10^{-12}$ ), suggesting a highly monotonic trend that denser topic graphs are generally less polarized. To facilitate a direct comparison between the two features despite different scales, Figure 1c overlays their min-max normalized relationships. Both features exhibit consistent decreasing trends with polarization, while  $\rho_{\pm}$  provides a particularly direct proxy for cross-camp mixing. We emphasize that these results are descriptive correlations across datasets rather than causal claims; nevertheless, they motivate treating cross-camp mixing and connectivity as informative global signals for characterizing polarization regimes in our experimental benchmark.

**Dataset filtering by initial polarization.** While Table 1 summarizes all 31 structurally valid topic graphs, our main experiments further focus on instances with sufficiently strong *initial* polarization. This additional filtering is motivated by two considerations. First, when the initial polarization is very small, the achievable reduction under any intervention budget is limited, which yields weak reward signals and makes learning-based methods difficult to train and evaluate fairly. Second, we aim to select a threshold that retains the majority of genuinely polarized scenarios while excluding graphs that are clearly weakly polarized. Consistent with the dataset-level correlation analysis in Fig. 1a–1c, higher

Table 2: Datasets retained after polarization-based filtering ( $\pi(\mathbf{z}^{(0)}) > 0.4$ ), sorted by number of nodes.

Dataset	num_nodes	initial_polarization	Dataset	num_nodes	initial_polarization
follow_germanwings	2111	0.444798	retweet_wcw	10674	0.989599
retweet_russia_march	2134	0.922033	retweet_onedirection	15292	0.682127
follow_mothersday	2225	0.605785	retweet_leadersdebate	25983	0.662604
retweet_nationalkissingday	4638	0.496141	retweet_jurassicworld	26407	0.910723
retweet_ff	5401	0.984460	retweet_germanwings	29763	0.842629
retweet_gunsense	7106	0.834818	retweet_nepal	40579	0.807100
retweet_ultralive	9261	0.595510	retweet_mothersday	155599	0.943096
retweet_sxsw	9304	0.930273			

Table 3: Summary statistics (min/mean/max) of key indicators on the filtered benchmark ( $\pi(\mathbf{z}^{(0)}) > 0.4$ ).

Metric	min	mean	max
avg_degree	2.076760	3.707899	12.728100
cross_community_ratio	0.001948	0.047577	0.237542
initial_polarization	0.444798	0.776780	0.989599

initial polarization tends to coincide with more pronounced echo-chamber structure (i.e., lower cross-camp exposure  $\rho_{\pm}$  and typically lower overall connectivity), so focusing on sufficiently polarized instances also emphasizes regimes where echo chambers are structurally clearer.

To make the filtering criterion comparable across datasets, we evaluate the initial polarization under the canonical extreme two-camp configuration, i.e., assigning internal opinions as  $s_i \in \{-1, +1\}$  according to the provided two-camp partition (with  $-1$  for one camp and  $+1$  for the other), and computing the corresponding settled opinions and initial polarization  $\pi(\mathbf{z}^{(0)})$ . We then keep only datasets with  $\pi(\mathbf{z}^{(0)}) > 0.4$ . This threshold balances coverage and difficulty: it retains most clearly polarized scenarios while excluding weakly polarized graphs where the achievable reduction (and thus the learning signal) is small. The resulting subset constitutes our final experimental benchmark, ensuring that all instances exhibit a clear polarization regime and that interventions produce informative learning signals. The retained datasets (sorted by number of nodes) are summarized in Table 2.

**Summary statistics of filtered datasets.** To characterize the structural regimes of the filtered benchmark, we additionally report summary statistics (min/mean/max) of three polarization-related indicators computed over the retained topic graphs: the average degree  $\bar{d}$ , the cross-camp edge ratio  $\rho_{\pm}$ , and the initial polarization  $\pi(\mathbf{z}^{(0)})$  under the extreme two-camp configuration. As shown in Table 3, the retained instances exhibit consistently low cross-camp mixing on average (mean  $\rho_{\pm} = 0.0476$ ), while spanning a wide range of connectivity (from sparse graphs with  $\bar{d} \approx 2.08$  to denser ones with  $\bar{d} \approx 12.73$ ). Overall, the high mean polarization (0.7768) confirms that this subset concentrates on clearly polarized (echo-chamber-like) regimes where intervention trajectories produce informative reward signals.

**Summary statistics of synthetic training/testing graphs.** In addition to the real-world benchmark, we also summarize the structural regimes covered by our *synthetic* two-echo-chamber graphs used for offline training and evaluation. Following Sec. 4.1, we generate two-community BA graphs, assign extreme camp opinions ( $\pm 1$ ) according to the planted partition, and then add sparse inter-community edges. Compared with the earlier synthetic setting, the current generator further applies an *initial-polarization filtering* step: a sampled graph is retained only if its initial polarization satisfies  $\pi(\mathbf{z}^{(0)}) \geq 0.4$ . This ensures that all synthetic instances used in training and testing lie in a sufficiently polarized regime and avoids weakly polarized cases with limited room for meaningful intervention.

For each node-size range, we report the number of generated graphs and the observed value ranges (min–max across graphs) of three indicators: average degree  $\bar{d}$ , cross-camp edge ratio  $\rho_{\pm}$ , and the resulting initial polarization  $\pi(\mathbf{z}^{(0)})$ .

As summarized in Table 4, the filtered synthetic graphs remain structurally consistent across all size ranges. The average degree now lies in a moderately denser regime, roughly from 3.56 to 15.81, while cross-camp exposure remains low by construction, typically between 0.00 and 0.12. Due to the explicit rejection step enforcing  $\pi(\mathbf{z}^{(0)}) \geq 0.4$ , all retained graphs exhibit clearly polarized initial states, with observed polarization ranges concentrated in  $[0.40, 1.00]$  up to minor range-specific variation.

Table 4: Per-range statistics of synthetic graphs used for training/testing. For each node-size range, we report the number of generated graphs and the min–max range of  $\bar{d}$ ,  $\rho_{\pm}$ , and  $\pi(\mathbf{z}^{(0)})$  under the extreme two-camp assignment after applying the initial-polarization filter  $\pi(\mathbf{z}^{(0)}) \geq 0.4$ .

range	n_graphs	avg_degree	cross_community_ratio	initial_polarization
30–50	100	3.56~10.98	0.00~0.11	0.40~1.00
50–100	100	3.72~13.49	0.01~0.12	0.40~0.94
100–200	100	3.89~14.78	0.01~0.11	0.40~0.92
200–300	100	3.97~15.38	0.01~0.11	0.40~0.92
300–400	100	4.01~15.58	0.01~0.11	0.40~0.89
400–500	100	4.00~15.81	0.01~0.11	0.40~0.93

Importantly, these filtered synthetic regimes are more closely aligned with the real-world filtered benchmark used in our main experiments, where we also focus on sufficiently polarized instances. Moreover, the per-range statistics remain highly stable as graph size increases from 30–50 to 400–500 nodes: although the upper bound of  $d$  grows moderately with size, the ranges of  $\rho_{\pm}$  and  $\pi(\mathbf{z}^{(0)})$  stay remarkably consistent. This suggests that the synthetic generator mainly controls the *polarization regime*—namely, within-camp connectivity, limited cross-camp mixing, and sufficiently high initial polarization—rather than producing size-specific distribution shifts. In particular, the training range (30–50) already exhibits the same low-mixing and high-polarization pattern as the larger test ranges, supporting inductive generalization from small training graphs to larger synthetic graphs.

## 5.2 Visualization Protocol and Evaluation Views

To provide a comprehensive and interpretable evaluation across intervention tasks and datasets, we report results using three complementary visualization views: *per-dataset bar charts*, *heatmap summaries*, and *polarization trajectories*.

**(1) Per-dataset bar charts (AUC / ANP summary).** For each task and each dataset, we report the accumulated normalized polarization (ANP) (or its AUC-style equivalent) as a single scalar performance metric. Lower values indicate better overall trajectory-aware performance. Bar charts allow direct horizontal comparison between methods on the same dataset, highlighting absolute gains and relative ranking.

**(2) Heatmap overview (cross-dataset consistency).** To visualize performance consistency across all datasets simultaneously, we present method  $\times$  dataset heatmaps. Each cell represents the ANP/AUC score of a method on a dataset. This view emphasizes vertical comparisons (how a method behaves across datasets) and horizontal comparisons (which datasets are intrinsically harder). Heatmaps make it easy to identify systematic advantages rather than isolated wins.

**(3) Polarization trajectories (temporal behavior).** Since our evaluation metric rewards early and persistent polarization reduction, we additionally visualize full intervention trajectories on representative datasets. Trajectory plots reveal *when* polarization reduction occurs, distinguishing methods that reduce polarization early from those that only improve near the budget limit. Better methods exhibit steeper early-stage decline and maintain lower curves throughout the horizon.

Together, these three views provide complementary perspectives: bar charts summarize final trajectory quality, heatmaps highlight cross-dataset robustness, and trajectories explain the temporal dynamics underlying AUC differences.

## 5.3 Baseline Methods

We compare PACIFIER against a set of analytical, heuristic, structural, and oracle-style baselines. Unless otherwise stated, all methods *without* the suffix **-FI** operate under the standard *one-shot planning* regime defined in Sec. 3.4: they must commit to a complete intervention sequence using only the initial instance information and are not allowed to use recomputed intermediate settled-opinion states during planning. Methods with the suffix **-FI** are their *full-information* counterparts: they are allowed to access recomputed settled-opinion states after each partial intervention step and can therefore replan sequentially using intermediate feedback.

**PACIFIER variants.** We evaluate two versions of the proposed method. **PACIFIER-RL** is the full reinforcement-learning variant, which learns long-horizon action values and performs sequential intervention by greedy decoding

of the learned  $Q$ -function. **PACIFIER-Greedy** shares the same encoder–decoder architecture but is trained only on immediate rewards, thus serving as a myopic learned ranking policy. Both variants follow the one-shot regime in the standard experiments. In the full-information comparison, we additionally consider **PACIFIER-RL-FI** and **PACIFIER-Greedy-FI**, which expose recomputed intermediate settled-opinion information to the same learned policies during sequential selection.

**BOMP.** **BOMP** (Binary Orthogonal Matching Pursuit) is the main analytical baseline for MI, following Matakos et al. [1]. It exploits the linear structure of the FJ steady-state solution and the associated global influence operator to iteratively select nodes whose internal-opinion neutralization is expected to most reduce polarization. **BOMP** is a strong reference in strictly linear MI settings, but its dense global computations become costly on large graphs and it is not naturally suited to topology-altering settings such as node removal.

**ExtremeExpressed.** **ExtremeExpressed** is a lightweight opinion-based heuristic that ranks candidate nodes according to the extremeness of their current expressed opinions. Intuitively, it prioritizes nodes whose expressed states are most polarized in magnitude, on the assumption that directly moderating such nodes yields strong immediate effect. In the standard one-shot setting, the ranking is determined from the initial settled-opinion state only. Its full-information counterpart, **ExtremeExpressed-FI**, recomputes the settled-opinion state after each intervention step and re-ranks the remaining candidates accordingly.

**ExtremeNeighbours.** **ExtremeNeighbours** is another opinion-aware heuristic that scores a node using the extremeness of its local neighborhood, aiming to identify nodes embedded in strongly polarized local environments. Compared with **ExtremeExpressed**, it injects a limited amount of neighborhood structure into the ranking rule, but still remains a simple non-learning baseline. As above, the standard version is one-shot, whereas **ExtremeNeighbours-FI** is the full-information version that recomputes the intermediate settled state and updates the ranking after each intervention step.

**PageRank.** **PageRank** is a purely structural baseline that ranks nodes by global graph centrality, independent of the current opinion state. It provides a strong topology-only reference for testing whether structural importance alone is sufficient for effective moderation. Because it does not depend on intermediate settled-opinion recomputation, we use **PageRank** only in its standard one-shot form in the main comparisons.

**Random.** **Random** selects nodes uniformly at random from the feasible set. It serves as a minimal baseline and helps quantify the extent to which all other methods improve over uninformed intervention.

**Cost.** **Cost** is a simple cost-only baseline used exclusively in the cost-weighted intervention tasks. It ranks all feasible nodes in ascending order of their intervention cost and directly selects the cheapest nodes as the intervention sequence, without using any opinion or structural information. This baseline serves to test whether performance in cost-aware settings can be explained merely by preferring low-cost nodes, rather than by reasoning jointly about cost, network structure, and opinion dynamics. Because its ranking depends only on the static node costs, we use **Cost** only in the standard one-shot form.

**Greedy (oracle-style full-information baseline).** In the synthetic full-information comparison, we additionally include **Greedy**, an oracle-style replanning baseline. At each step, it exhaustively tries every feasible candidate node, temporarily applies the intervention, recomputes the resulting settled-opinion state, evaluates the immediate polarization reduction, rolls the intervention back, and then selects the best candidate. This method explicitly uses intermediate settled-opinion information and therefore belongs to the full-information regime. It is computationally expensive but provides a strong upper-level myopic reference for understanding the value of sequential replanning with explicit feedback.

**One-shot vs. full-information distinction.** The distinction between one-shot and full-information baselines is central to our evaluation. One-shot methods are constrained to plan from the initial instance only and therefore match the practical deployment regime targeted by **PACIFIER**. By contrast, full-information methods are allowed to repeatedly recompute intermediate settled-opinion states and update their decisions online. Our standard experiments compare **PACIFIER** against one-shot baselines, while the dedicated full-information synthetic benchmark separately examines how much additional benefit can be obtained when such intermediate feedback is made available.

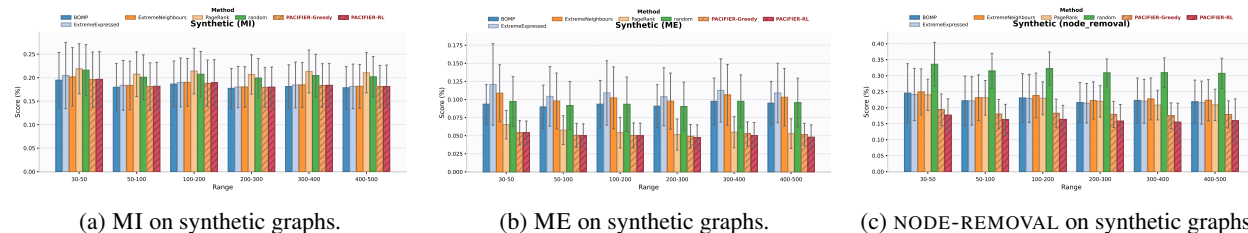


Figure 2: Synthetic benchmark results across six node-size ranges (30–50, 50–100, 100–200, 200–300, 300–400, 400–500), with 100 graphs per range. Bars compare PACIFIER with all baselines on three tasks: MI, ME, and NODE-REMOVAL. The score represented by each bar height is the ANP score reported in this paper, and lower values indicate better performance.

#### 5.4 Synthetic Benchmark: Performance across Graph Sizes

We further evaluate PACIFIER on a controlled *synthetic* benchmark to examine generalization across graph sizes and to provide an apples-to-apples comparison with competing methods under identical instance distributions. We generate two-echo-chamber graphs following the procedure in Sec. 4.1, and report results on six node-size ranges: {30–50, 50–100, 100–200, 200–300, 300–400, 400–500}. For each size range, we sample 100 graphs, resulting in 600 test instances in total. We compare PACIFIER against all baselines on three tasks: MI, ME, and NODE-REMOVAL. In each bar chart, the x-axis denotes the node-size range, and each bar reports the average score over the 100 graphs in that range, with error bars indicating the standard deviation when available.

**Discussion.** As shown in Fig. 2, the synthetic benchmark reveals three distinct behavioral regimes across tasks, which together clarify when simple myopic reasoning is sufficient and when long-horizon reinforcement learning becomes essential.

**(1) MI: PACIFIER matches the linear-model optimum.** From Fig. 2a, we observe that on the canonical MI task, both **PACIFIER-RL** and **PACIFIER-Greedy** achieve performance very close to **BOMP**, the classical model-aware algorithm that explicitly exploits the linear structure of the FJ steady-state solution. Across all graph-size ranges from 30–50 up to 400–500, the two PACIFIER variants closely track the BOMP curve and consistently outperform structural heuristics such as PageRank, ExtremeExpressed, ExtremeNeighbours, and random selection. This indicates that the learned representation successfully captures the same influence structure that BOMP leverages analytically, despite not relying on closed-form matrix operations at deployment time. Moreover, the negligible gap between PACIFIER-RL and PACIFIER-Greedy suggests that in this linear and comparatively well-structured setting, the immediate polarization-reduction signal is already well aligned with the long-term objective. As a result, myopic value estimation is sufficient to recover near-optimal action rankings.

**(2) ME: RL shows stronger scale generalization than Greedy on synthetic graphs.** In contrast, Fig. 2b shows a markedly different pattern for ME. Here, **PACIFIER-RL** consistently achieves the best performance across all graph sizes, while **PACIFIER-Greedy** is noticeably weaker and remains much closer to the stronger classical baselines. Relative to Greedy, RL exhibits clearly stronger scale generalization on the synthetic benchmark, that is, under matched synthetic training and test distributions without considering the training-distribution gap that may arise on real datasets. The gap between RL and Greedy is persistent rather than incidental, indicating that once interventions operate on expressed opinions, the action value can no longer be inferred reliably from immediate single-step gains alone. Fixing a node’s expressed opinion changes not only the current equilibrium, but also the downstream feasibility and utility of future interventions, creating strong sequential dependencies. Such effects are difficult to capture with purely myopic regression, but are naturally handled by bootstrapped Q-learning. The stability of this RL-over-Greedy advantage across all six graph-size ranges therefore suggests that long-horizon credit assignment is important for ME-style interventions rather than being only a small-graph artifact.

**(3) Node-removal: RL clearly outperforms Greedy.** Fig. 2c presents an even clearer regime. For NODE-REMOVAL, **PACIFIER-RL** achieves the lowest score in every size range, with a consistent margin over all baselines. At the same time, **PACIFIER-Greedy** remains the second-best method overall and also substantially outperforms BOMP, PageRank, ExtremeExpressed, ExtremeNeighbours, and random selection. More importantly, RL is clearly better than Greedy in this setting. Compared with MI, this larger RL–Greedy gap suggests that node-removal introduces stronger combinatorial and long-range intervention effects: removing one node can fundamentally alter the subsequent graph topology, influence pathways, and the marginal utility of later actions. Therefore, while myopic learning already

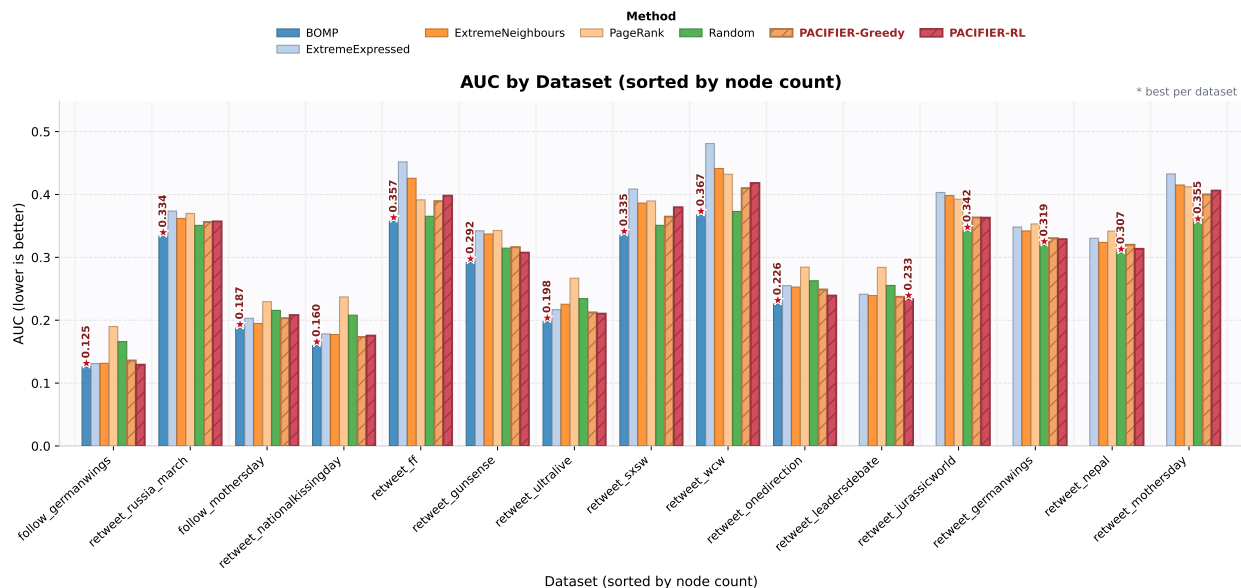


Figure 3: Real datasets (MI): per-dataset bar comparison (lower is better).

captures useful local signals, full reinforcement learning is much better suited to reasoning over the nonlinear sequential consequences induced by structural interventions.

**(4) Scalability and regime-dependent optimality.** Across all three subfigures in Fig. 2, the relative ordering between methods remains highly stable as the graph size increases from 30–50 nodes to 400–500 nodes. This demonstrates strong inductive generalization from smaller training graphs to substantially larger synthetic instances. Taken together, the results reveal a clear regime-dependent picture: when the task admits a strong linear analytical structure as in MI, PACIFIER recovers near-optimal behavior comparable to BOMP. When interventions induce stronger sequential or structural dependencies, as in ME and especially NODE-REMOVAL, long-horizon reinforcement learning provides clear and consistent gains.

## 5.5 Real-world Datasets

We report results on the real-world polarized topic graphs described in Sec. 5.1. We focus on three representative intervention settings: the two canonical topology-preserving tasks, **MI** and **ME**, and the topology-altering setting **node\_removal**. For each task, we provide: (i) a per-dataset bar chart summarizing the ANP/AUC-style metric, (ii) a heatmap overview across datasets and methods, and (iii) representative polarization trajectories illustrating *when* polarization reduction occurs along the intervention horizon.

**Per-dataset bar charts.** The following bar charts compare **PACIFIER** with all baselines on each dataset. Lower values indicate better trajectory-aware performance (area-under-curve / accumulated metric).

**Heatmap overview.** Heatmaps provide a compact view of method performance across all datasets, highlighting relative strengths and weaknesses under different intervention settings.

**Trajectory curves (representative datasets).** To qualitatively illustrate *when* polarization reduction happens along the intervention horizon, we visualize polarization trajectories on **three representative datasets** for each task. Specifically, we select (i) the dataset with the smallest number of nodes, (ii) the largest dataset whose size is below a threshold (e.g.,  $n < 20,000$ ), and (iii) the dataset with the largest number of nodes. This selection covers small/medium/large regimes while keeping the main text concise. The complete set of trajectory plots for all datasets is provided in the Appendix.

### 5.5.1 Discussion

We next analyze the real-world results in detail. For each intervention setting (MI, ME, and node\_removal), we discuss the empirical findings from three complementary perspectives: (i) per-dataset bar comparisons, (ii) heatmap-level

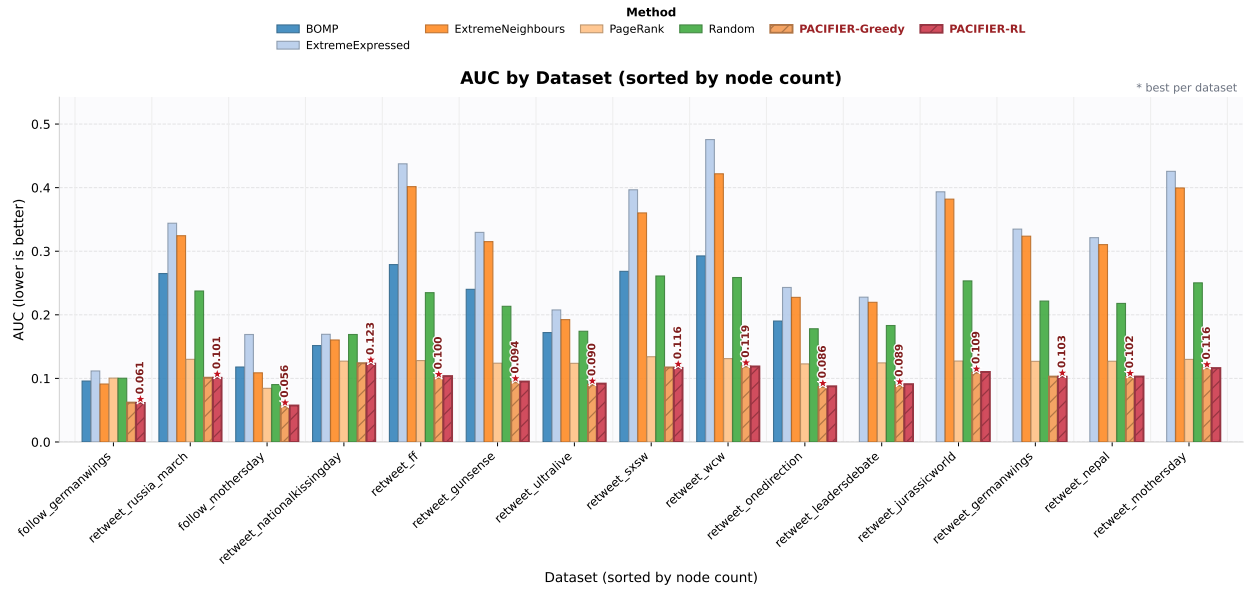


Figure 4: Real datasets (ME): per-dataset bar comparison (lower is better).

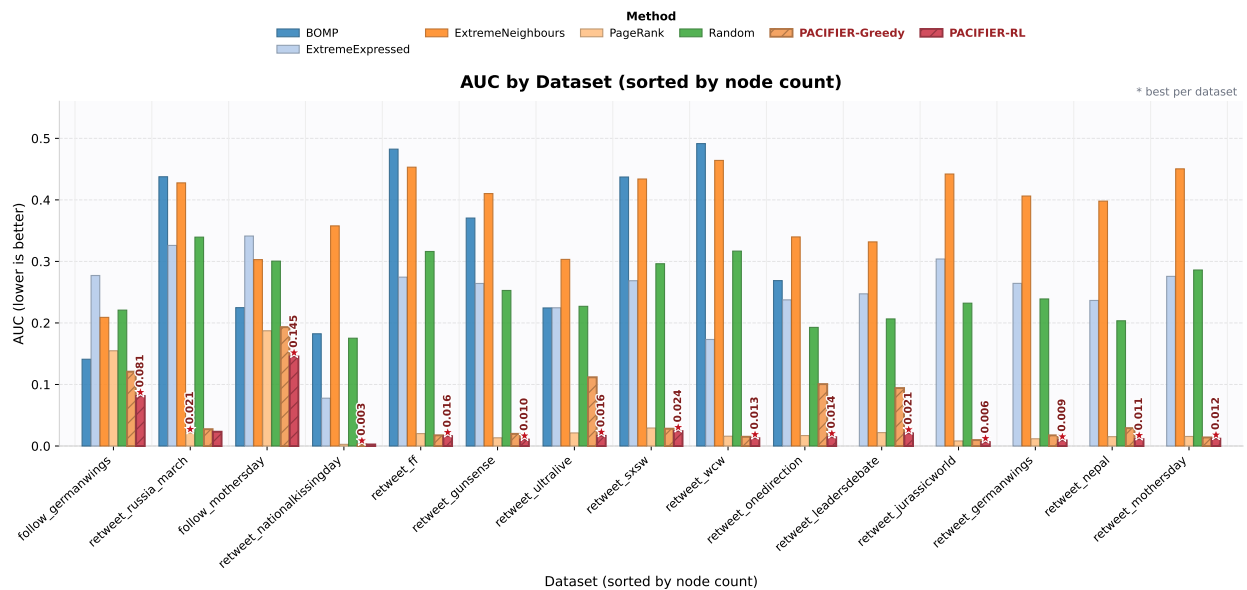


Figure 5: Real datasets (node\_removal): per-dataset bar comparison (lower is better).

performance patterns across datasets, and (iii) representative polarization trajectories that reveal the temporal evolution of polarization. Together, these three tasks allow us to compare PACIFIER across both topology-preserving and topology-altering regimes.

**Evaluation protocol note.** Across all three real-world tasks (MI, ME, and **node\_removal**), we evaluate on the same set of 15 polarized topic graphs. However, **BOMP** is only available on 10 of these 15 datasets, because its computation becomes prohibitively expensive on the five largest graphs. As a result, any average reported for BOMP is computed on this 10-dataset subset only, and is therefore not directly comparable to averages of methods such as PACIFIER that are reported over all 15 datasets. Accordingly, in the task-specific discussion below, we distinguish subset-based average comparisons from full-coverage results, and we place primary emphasis on per-dataset comparisons against the strongest available non-PACIFIER baseline.

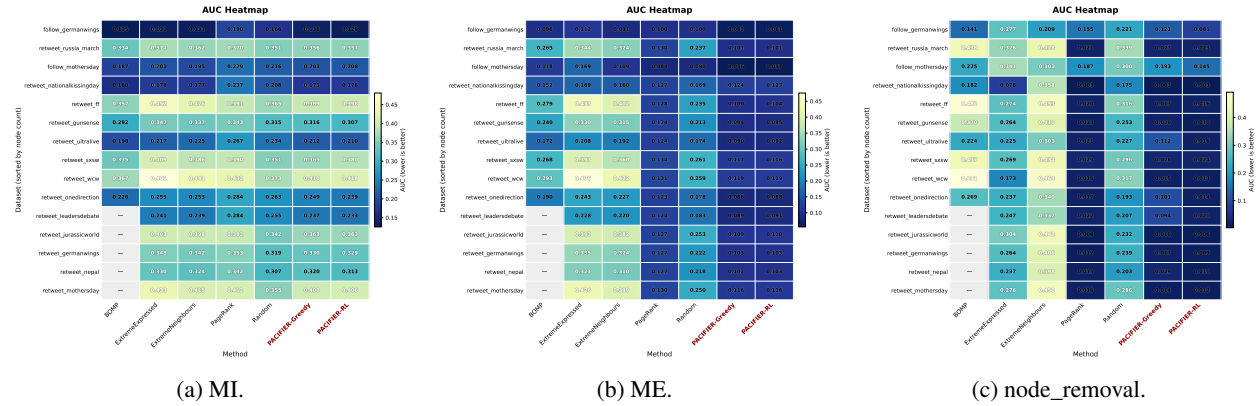


Figure 6: Real datasets: heatmap summaries for MI, ME, and node\_removal. Lower is better.

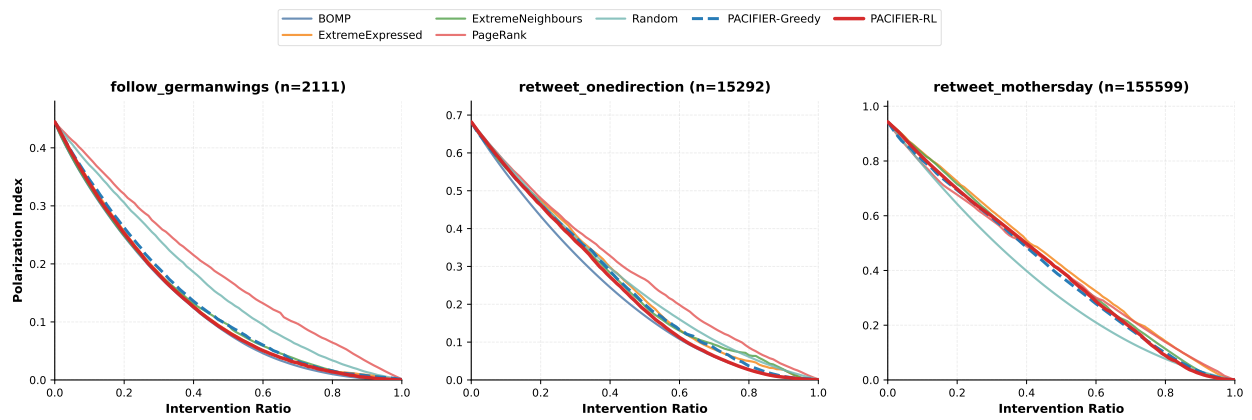


Figure 7: Real datasets (MI): polarization trajectories on three representative datasets (small / medium / large by node count). Lower and earlier is better. Full trajectories for all datasets are in the Appendix.

**MI.** On the real-world MI benchmark, PACIFIER does not surpass BOMP when the latter is computationally feasible, which is expected since MI is precisely the regime where analytical structure is the cleanest and BOMP can be regarded as the strongest classical solver. In this sense, the real-world MI results should not be interpreted as a failure of the framework, but rather as a test of how much of this analytical decision structure PACIFIER can recover from synthetic training and transfer to heterogeneous real graphs.

As noted above, BOMP is only available on 10 out of the 15 real-world datasets, because its computation becomes prohibitively expensive on the five largest graphs. On this 10-dataset BOMP-comparable subset, BOMP remains the strongest method on average, achieving an average AUC of 0.258. PACIFIER-Greedy and PACIFIER-RL obtain average AUCs of 0.281 and 0.282, respectively, and neither variant outperforms BOMP on any of these 10 datasets. This confirms that, in the canonical linear MI regime, the strongest analytical solver still retains a clear advantage whenever it is available.

At the same time, these results also suggest a mild but non-negligible synthetic-to-real gap. Although our synthetic graph generator explicitly uses two echo chambers to better align with the opposing-camp structure observed in polarized real networks, this approximation is still not sufficient to fully match the heterogeneity of real MI instances. As a result, PACIFIER can recover a substantial portion of the useful decision structure learned in synthetic environments, but transferring that behavior to real-world graphs remains somewhat imperfect.

However, since BOMP is already effectively the strongest classical reference for MI, the more practically relevant comparison is between PACIFIER and the remaining scalable non-PACIFIER baselines. Under this excluding-BOMP view, the picture becomes substantially more favorable to PACIFIER. On the same 10-dataset subset, PACIFIER-Greedy is the best method on average among all non-BOMP methods (0.281), with PACIFIER-RL a close second (0.282), both outperforming Random (0.284) and the other heuristic baselines on average. At the dataset level, PACIFIER-RL outperforms the strongest excluding-BOMP baseline on 5 out of 10 datasets, while PACIFIER-Greedy does so on 3 out

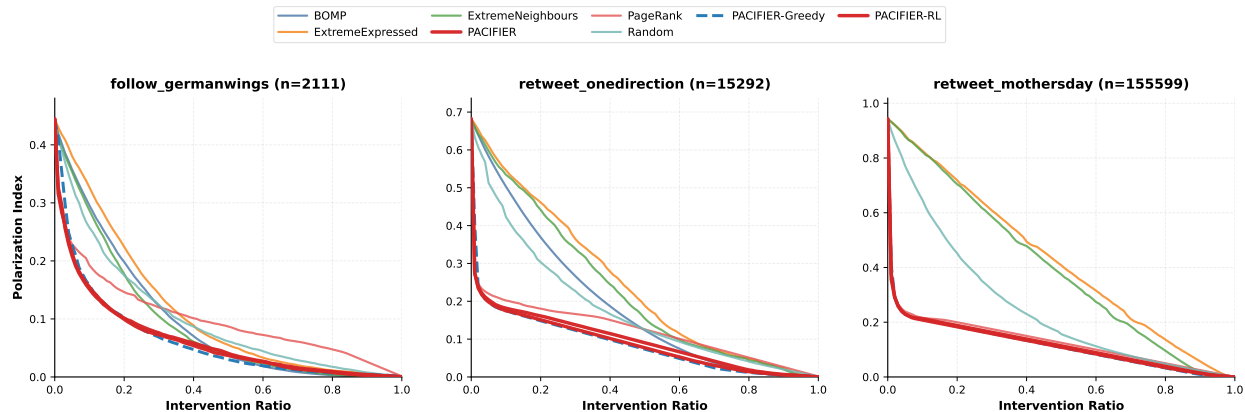


Figure 8: Real datasets (ME): polarization trajectories on three representative datasets (small / medium / large by node count). Lower and earlier is better. Full trajectories for all datasets are in the Appendix.

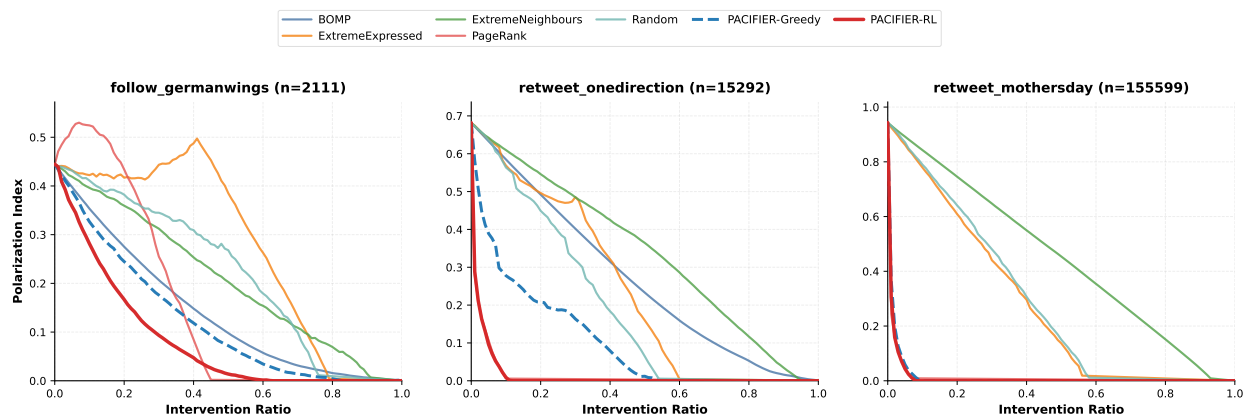


Figure 9: Real datasets (node\_removal): polarization trajectories on three representative datasets (small / medium / large by node count). Lower and earlier is better. Full trajectories for all datasets are in the Appendix.

of 10, with mean relative gaps of only 2.51% and 2.49%, respectively. This indicates that although PACIFIER does not match BOMP, it already becomes highly competitive once the comparison is restricted to non-analytical baselines.

The same pattern also appears under the full-coverage evaluation that excludes BOMP and uses all 15 datasets. In this setting, Random is the strongest baseline on average with an AUC of 0.295, while PACIFIER-Greedy and PACIFIER-RL achieve 0.297 and 0.298, respectively. Relative to the strongest available excluding-BOMP baseline on each dataset, PACIFIER-RL wins on 6 out of 15 datasets and PACIFIER-Greedy wins on 4 out of 15, with mean relative gaps of 3.21% and 3.37%, respectively. Thus, even though a synthetic-to-real transfer gap remains, the gap is moderate rather than severe when PACIFIER is compared against the scalable baselines that are actually available across the full benchmark.

Several representative datasets further support this interpretation. On *follow\_germanwings*, PACIFIER-RL ranks second overall behind BOMP (0.129 vs. 0.125), and it also outperforms the strongest excluding-BOMP baseline, *ExtremeExpressed* (0.129 vs. 0.131). On *retweet\_onedirection*, PACIFIER-RL is again second only to BOMP (0.239 vs. 0.226), while outperforming the strongest excluding-BOMP baseline, *ExtremeNeighbours* (0.239 vs. 0.253). At the same time, difficult cases such as *retweet\_mothersday* show that this transfer remains non-trivial on highly heterogeneous large-scale graphs.

Overall, the MI results are best interpreted as evidence of a meaningful but bounded transfer gap. BOMP remains the strongest method whenever it is feasible, which is consistent with MI being the most analytically structured setting. But once the focus shifts to the more practical comparison against scalable non-PACIFIER baselines, PACIFIER becomes highly competitive: it is among the best methods on average, wins on a substantial fraction of datasets, and clearly preserves a significant portion of the useful decision structure learned from synthetic training.

**ME.** The real-world results under the ME objective are substantially stronger than those under MI. Rather than merely remaining competitive, PACIFIER consistently outperforms all classical non-PACIFIER baselines across the benchmark. This suggests that ME is a regime in which the intervention policy learned from synthetic graphs transfers to real networks particularly well, and where classical analytical or structural heuristics no longer define the performance frontier.

This conclusion already holds on the 10-dataset subset where BOMP is computationally feasible. On this subset, PACIFIER-Greedy and PACIFIER-RL achieve average AUCs of 0.0949 and 0.0956, respectively, clearly outperforming the strongest non-PACIFIER baseline, PageRank, at 0.1205, and also substantially outperforming BOMP at 0.2073. At the dataset level, both PACIFIER variants outperform the strongest non-PACIFIER baseline on all 10 datasets: PACIFIER-Greedy achieves a 10/10 win rate with a mean relative improvement of 21.55%, and PACIFIER-RL also achieves a 10/10 win rate with a mean relative improvement of 20.96%. Therefore, unlike MI, ME does not appear to be a setting where analytical baselines retain a decisive real-world advantage.

At the same time, the relationship between PACIFIER-RL and PACIFIER-Greedy is also informative. On fully aligned synthetic benchmarks, where the training and test distributions match closely, RL exhibits stronger scale generalization than Greedy, indicating that long-horizon reasoning is indeed beneficial for ME-style interventions. However, once the evaluation moves to real graphs, a mild synthetic-to-real gap still remains. Even though the synthetic generator is designed to better align with polarized real networks, real ME instances still contain additional heterogeneity that is not perfectly captured by the synthetic distribution. This gap is not large enough to undermine transfer, but it does appear to compress the difference between the two PACIFIER variants: RL and Greedy remain very close on real data, with Greedy even slightly outperforming RL on the current benchmark.

The same pattern becomes even clearer under the full-coverage comparison that excludes BOMP and uses all 15 datasets. In this setting, PACIFIER-Greedy and PACIFIER-RL obtain average AUCs of 0.0978 and 0.0986, respectively, while PageRank, the strongest non-PACIFIER baseline on average, reaches 0.1227. More importantly, both PACIFIER variants outperform the strongest available non-PACIFIER baseline on every dataset in the benchmark. PACIFIER-Greedy achieves a 15/15 win rate with a mean relative improvement of 20.52%, and PACIFIER-RL also achieves a 15/15 win rate with a mean relative improvement of 19.90%. This dominance is also highly stable across graph sizes: in the small, medium, and large buckets, both variants maintain a 100% win rate, with mean gains remaining consistently around 18%–23%.

Representative datasets further illustrate this robustness. On *follow\_germanwings*, both PACIFIER variants dramatically outperform the strongest baseline, *ExtremeNeighbours*, with PACIFIER-RL achieving 0.0613 and PACIFIER-Greedy 0.0619 versus 0.0911. On *retweet\_onedirection*, both again show a large advantage over PageRank, with PACIFIER-Greedy and PACIFIER-RL obtaining 0.0864 and 0.0876, compared with 0.1228. Even on the very large *retweet\_mothersday* graph, where the task is more challenging and the synthetic-to-real mismatch is likely more pronounced, PACIFIER-Greedy and PACIFIER-RL still clearly outperform PageRank (0.1159 and 0.1162 versus 0.1299). These examples indicate that the learned intervention strategy transfers robustly not only on small graphs, but also on large and heterogeneous real networks.

Overall, ME provides some of the clearest evidence of successful synthetic-to-real transfer in our framework. In fully aligned synthetic settings, RL shows stronger scale generalization than Greedy, confirming the value of long-horizon reasoning for this objective. On real-world graphs, a mild transfer gap remains, but it does not change the qualitative conclusion: both PACIFIER variants remain highly effective, perform very similarly to each other, and consistently dominate all non-PACIFIER baselines across the benchmark.

**Node removal.** The real-world results on the *node\_removal* task provide strong evidence that explicit sequential decision-making is necessary for effective intervention. Unlike ME, where PACIFIER-RL and PACIFIER-Greedy remain very close on real graphs, here PACIFIER-RL clearly separates itself not only from the classical baselines, but also from PACIFIER-Greedy. This suggests that *node\_removal* is inherently more sensitive to long-horizon credit assignment: removing a node changes the future graph structure directly, and the quality of later decisions therefore depends strongly on the earlier intervention sequence.

This conclusion already holds on the 10-dataset subset where BOMP is computationally feasible. On this subset, PACIFIER-RL is the best method on average, achieving an average AUC of 0.0346, compared with 0.0483 for PageRank, 0.0636 for PACIFIER-Greedy, and 0.3261 for BOMP. At the dataset level, PACIFIER-RL outperforms the strongest available non-PACIFIER baseline on 9 out of 10 datasets, with a mean relative improvement of 18.02%. By contrast, PACIFIER-Greedy wins on only 5 out of 10 datasets, and its mean relative improvement is strongly negative overall due to several severe failure cases. Therefore, unlike MI, BOMP is not a competitive reference in this setting, and unlike ME, the gap between RL and Greedy remains clearly visible even on real-world graphs.

The same pattern becomes even clearer under the full-coverage comparison that excludes BOMP and uses all 15 datasets. In this setting, PACIFIER-RL again ranks first on average with an AUC of 0.0270, clearly outperforming PageRank, the strongest non-PACIFIER baseline, at 0.0370. More importantly, PACIFIER-RL outperforms the strongest available non-PACIFIER baseline on 14 out of 15 datasets, with a mean relative improvement of 19.16%. In contrast, PACIFIER-Greedy achieves an average AUC of 0.0534, wins on only 6 out of 15 datasets, and exhibits a strongly negative mean relative improvement overall because of several pronounced failure cases. This shows that the advantage of PACIFIER in *node\_removal* is not merely due to using a learned scoring function, but specifically due to the RL policy’s ability to reason over the downstream structural consequences of each intervention step.

The bucketed analysis further supports this interpretation. PACIFIER-RL remains strong across all graph sizes: it wins on 3 out of 4 small graphs, 5 out of 5 medium graphs, and 6 out of 6 large graphs, with mean relative improvements of 16.80%, 20.42%, and 19.68%, respectively. Thus, its advantage is not confined to a particular scale, but persists from small real networks to the largest graphs in the benchmark. By contrast, PACIFIER-Greedy becomes increasingly unstable as graph size grows: while it remains partially competitive on small and medium graphs, it wins on only 1 out of 6 large graphs and suffers especially large degradations on several medium- and large-scale instances. This contrast strongly suggests that scale generalization in *node\_removal* depends crucially on true sequential planning rather than myopic ranking quality alone.

Representative datasets illustrate the same pattern. On *follow\_germanwings*, PACIFIER-RL achieves the best overall result, substantially outperforming both BOMP and PageRank (0.0811 vs. 0.1410 and 0.1548), while PACIFIER-Greedy remains competitive but clearly weaker at 0.1208. On *retweet\_onedirection*, PACIFIER-RL again ranks first and improves over PageRank by 15.98% (0.0143 vs. 0.0170), whereas PACIFIER-Greedy deteriorates sharply to 0.1006. Even on the extremely large *retweet\_mothersday* graph, PACIFIER-RL still achieves the best result at 0.0119, outperforming PageRank at 0.0155, while PACIFIER-Greedy remains competitive but still trails RL at 0.0139. These cases show that the RL advantage is both substantial and robust, although Greedy can still recover useful behavior on some large instances.

Overall, the *node\_removal* results provide strong evidence that PACIFIER-RL has learned a genuinely transferable sequential intervention policy rather than a simple static heuristic. The synthetic-to-real gap does not disappear completely, but it is clearly small enough for the RL policy to transfer very effectively across heterogeneous real graphs. At the same time, the persistent gap between RL and Greedy indicates that for *node\_removal*, unlike ME, real-world performance depends critically on modeling the long-term interaction between current interventions and future graph evolution.

## 5.6 Real-world Datasets in Extended Settings

We further report results on the same real-world polarized topic graphs under two extended settings: **continuous** and **cost**. Each setting contains two topology-preserving intervention tasks, namely **MI** and **ME**. To keep the presentation concise and focused, we report only the per-dataset bar charts for these extended settings. These figures summarize the trajectory-aware performance across datasets using the same ANP/AUC-style metric as in the main experiments, where lower values indicate better performance.

### 5.6.1 Continuous Setting

**Per-dataset bar charts.** The following bar charts compare **PACIFIER** with all baselines on each dataset under the continuous-opinion setting. Lower values indicate better trajectory-aware performance (area-under-curve / accumulated metric).

**Discussion.** We next analyze the real-world results under the continuous-opinion setting. Unlike the main real-world benchmark in Sec. 5.5, here we report only per-dataset bar comparisons, so the discussion focuses on cross-dataset performance patterns visible from these bars, together with subset-based summary statistics when **BOMP** is only partially available.

**Evaluation protocol note.** As in the main real-world experiments, all continuous-setting results are evaluated on the same 15 polarized topic graphs. However, **BOMP** remains only partially available due to its computational cost on larger instances, and its coverage differs by task. For continuous-MI, BOMP is available on 10 of the 15 datasets; for continuous-ME, BOMP is available on 10 of the 15 datasets. Therefore, whenever BOMP is discussed, its averages should be interpreted only on the corresponding BOMP-comparable subset, rather than as directly comparable to full-coverage averages of methods such as PACIFIER. Accordingly, in the task-specific discussion below, we distinguish (i) comparisons on the BOMP-comparable subset and (ii) comparisons on the full dataset collection excluding BOMP from the strongest-baseline reference.

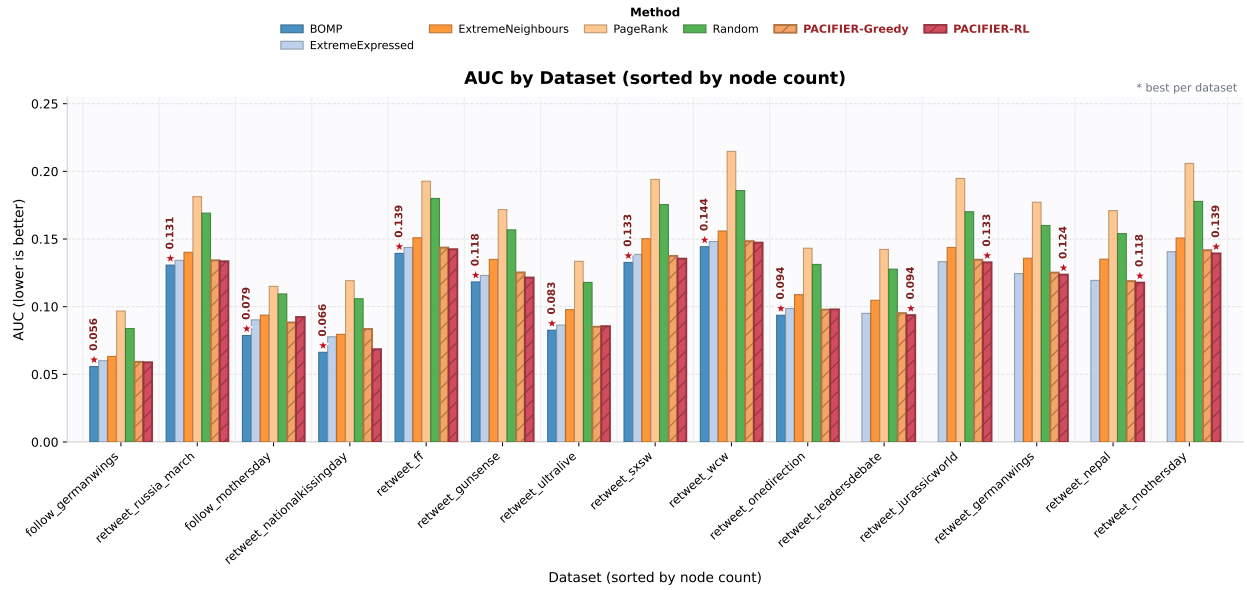


Figure 10: Real datasets (continuous-MI): per-dataset bar comparison (lower is better).

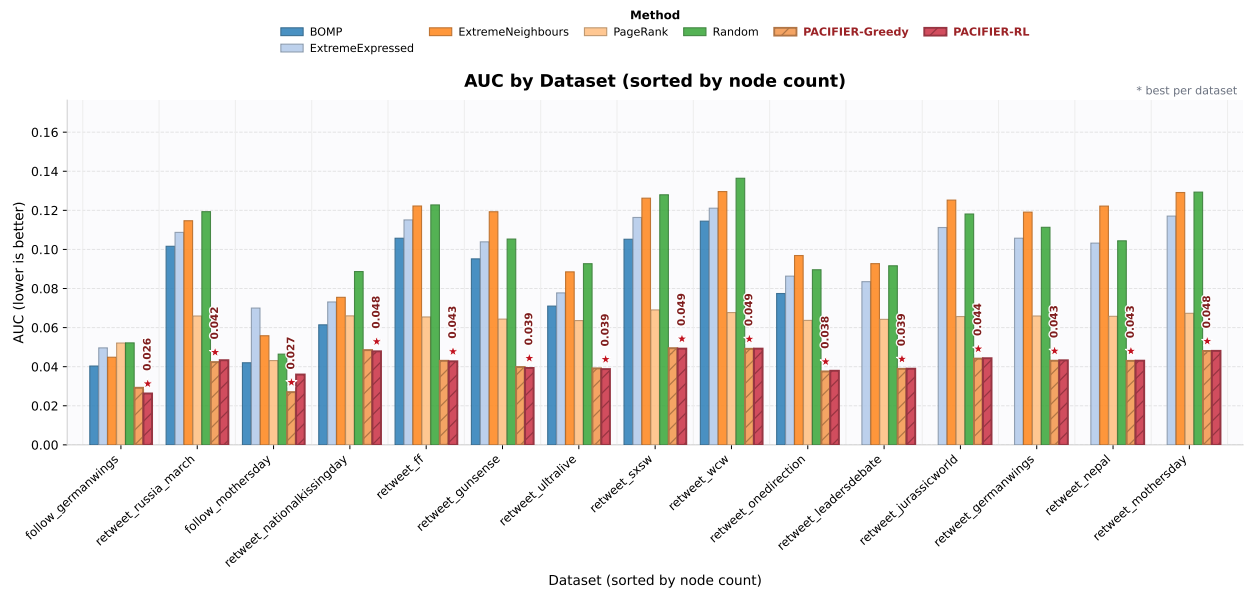


Figure 11: Real datasets (continuous-ME): per-dataset bar comparison (lower is better).

**Continuous-MI.** The continuous-MI results largely preserve the same high-level pattern observed in the canonical real-world MI benchmark: when the task remains close to the analytically structured internal-opinion moderation regime, **BOMP** continues to be the strongest available baseline whenever it is computationally feasible. This indicates that introducing continuous-valued internal opinions does not remove the core structural advantage enjoyed by a solver that is explicitly tailored to the linear influence operator.

More specifically, on the 10-dataset BOMP-comparable subset, **BOMP** achieves the best average AUC (0.104), while **PACIFIER-RL** and **PACIFIER-Greedy** obtain average AUCs of 0.108 and 0.110, respectively. Neither PACIFIER variant outperforms the strongest available non-PACIFIER baseline on any of these 10 datasets. This confirms that in continuous-MI, just as in the original MI setting, the analytically informed baseline remains difficult to surpass when its computation is still affordable.

At the same time, the comparison to the non-continuous benchmark reveals an important shift in the competitive landscape. In the original binary-opinion MI experiments, once **BOMP** and **PACIFIER** were excluded, the strongest remaining baseline was often simply **Random**, indicating that the lightweight classical heuristics contributed relatively little beyond the dominant analytical solver. By contrast, in the continuous-MI setting, the two opinion-aware heuristics **ExtremeExpressed** and **ExtremeNeighbours** become substantially more competitive and consistently rank among the strongest non-**PACIFIER** baselines. This is a meaningful change: it suggests that when internal opinions are no longer restricted to the extreme binary values  $\{-1, +1\}$  but instead vary continuously in magnitude, the classical opinion-sensitive ranking rules become more informative and effective.

This observation is important conceptually. It indicates that the moderation ideas underlying the classical methods introduced in the prior polarization literature remain valid in the continuous regime. In particular, once opinion strength becomes heterogeneous rather than purely binary, ranking rules based on opinion extremeness or locally polarized neighborhood structure can better exploit this additional signal. Thus, the continuous benchmark should not be interpreted as a setting where classical methods collapse; on the contrary, it is a setting where several of them become stronger competitors.

Against this stronger baseline landscape, **PACIFIER** still remains highly competitive. Although **PACIFIER-RL** does not surpass **BOMP** on the BOMP-comparable subset, the absolute gap is modest, whereas **PACIFIER-Greedy** falls somewhat further behind. This again suggests that long-horizon learned planning is able to recover a substantial part of the useful decision structure, even if it does not fully match the explicit analytical guidance available to **BOMP** in this regime.

From a practical perspective, the more relevant comparison is again against the scalable non-**PACIFIER** baselines excluding **BOMP**. Under this view, the picture becomes more favorable to **PACIFIER**. Across all 15 datasets, **PACIFIER-RL** outperforms the strongest available non-**PACIFIER** baseline on 14 of 15 datasets, with a positive mean improvement of 1.55%. Its advantage is modest but highly consistent, indicating that once the strongest analytical solver is removed from consideration, the learned RL policy becomes the most reliable overall method in the continuous-MI setting. By contrast, **PACIFIER-Greedy** is much less stable: it wins on only 7 of the 15 datasets and is essentially tied on average with the strongest non-**PACIFIER** competitor (mean improvement  $-0.33\%$ ).

This contrast between the two **PACIFIER** variants is also informative. Since the classical opinion-aware heuristics become stronger in the continuous regime, a purely myopic learned ranking policy is no longer sufficient to obtain a clear advantage. **PACIFIER-RL**, however, still manages to stay ahead on almost all datasets, which suggests that modeling longer-horizon interactions remains useful even when the handcrafted heuristics themselves become more competitive. Taken together, these results suggest a clear conclusion for continuous-MI: the task remains analytically structured enough that **BOMP** retains an advantage when available, the classical opinion-aware baselines from prior work also become meaningfully stronger than in the binary setting, and yet **PACIFIER-RL** still emerges as the strongest scalable non-analytical method overall.

**Continuous-ME.** The continuous-ME results are markedly more favorable to **PACIFIER** and, in fact, reveal an even cleaner picture than in the corresponding MI setting. Here, both learned **PACIFIER** variants dominate the non-**PACIFIER** baselines not only under the full-dataset excluding-**BOMP** comparison, but also on the stricter BOMP-comparable subset. This indicates that once the moderation target shifts from internal opinions to expressed opinions under continuous-valued states, the learned policies are able to exploit sequential intervention structure more effectively than the available analytical or heuristic alternatives.

On the 10-dataset BOMP-comparable subset, both **PACIFIER-RL** and **PACIFIER-Greedy** outperform the strongest available non-**PACIFIER** baseline on all 10 datasets. Their mean improvements are 31.45% and 32.77%, respectively, which is a very large margin for a real-world benchmark of this scale. Moreover, both variants achieve average AUC values around 0.041, substantially lower than **PageRank** (0.062), **BOMP** (0.081), and the opinion-based heuristics **ExtremeExpressed** and **ExtremeNeighbours**. This shows that in continuous-ME, **PACIFIER** does not merely remain competitive with classical methods; it clearly surpasses them, including **BOMP** on the subset where **BOMP** is still computationally feasible.

The same conclusion becomes even stronger under the full 15-dataset comparison excluding **BOMP**. Both **PACIFIER** variants achieve a 100% win rate against the strongest available non-**PACIFIER** baseline. **PACIFIER-RL** attains a mean improvement of 33.20%, while **PACIFIER-Greedy** achieves an even slightly larger 34.16%. This near-uniform dominance indicates that the continuous-ME task is especially well aligned with the type of sequential planning learned by **PACIFIER**. Unlike in MI, where analytical structure remains highly beneficial, in ME the main challenge is less about approximating a closed-form global influence operator and more about identifying effective intervention orderings under dynamic expressed-opinion responses. That is precisely the regime where learned planning appears most advantageous.

Another notable observation is that the two PACIFIER variants are extremely close to each other in continuous-ME, with **PACIFIER-Greedy** even slightly outperforming **PACIFIER-RL** on average. This suggests that, in this setting, much of the benefit may already be captured by a strong learned myopic ranking policy, and the additional long-horizon value modeling of RL does not produce a large extra gain. In other words, continuous-ME seems to be a regime where learning good action priorities is more important than explicitly modeling deep future dependencies. This behavior is qualitatively consistent with the strong performance of PACIFIER-Greedy in the original real-world ME benchmark as well.

The cross-dataset consistency is also particularly striking. On both the BOMP-comparable subset and the full dataset collection, PACIFIER maintains perfect win rates, and the improvement margins remain large rather than marginal. This indicates that the advantage is not driven by only a few favorable graphs, but reflects a systematic performance gap across heterogeneous real-world datasets. Overall, the continuous-ME benchmark provides some of the strongest evidence in the paper for the usefulness of the PACIFIER framework: under continuous-valued expressed-opinion moderation, the learned policies transfer robustly from synthetic training graphs to real-world networks and decisively outperform all non-PACIFIER baselines.

**Overall picture in the continuous setting.** Taken together, the continuous-setting results reveal a clear task-dependent pattern that both mirrors and sharpens the conclusions from the main benchmark. For continuous-MI, the problem remains sufficiently aligned with the analytically structured internal-opinion regime that **BOMP** continues to be the strongest method whenever it is available. At the same time, compared with the binary-opinion benchmark, the classical opinion-aware heuristics become substantially more competitive, showing that prior moderation ideas based on opinion extremeness and local polarized structure remain effective once continuous opinion magnitudes are introduced. Even under this stronger competitive landscape, **PACIFIER-RL** still stands out as the strongest scalable non-analytical alternative.

For continuous-ME, by contrast, both PACIFIER variants achieve strong and highly consistent superiority across all real-world datasets, including the subset where BOMP is still available. This contrast further supports the central claim of the paper: PACIFIER is especially effective in moderation settings where sequential decision structure dominates and where handcrafted analytical solvers no longer fully capture the relevant intervention dynamics. At the same time, the continuous-MI results also show that PACIFIER does not rely on weak baselines for its competitiveness: even when classical methods become stronger in the continuous regime, the framework remains robust and competitive, with **PACIFIER-RL** continuing to deliver the best overall performance among scalable learned or heuristic alternatives.

### 5.6.2 Cost Setting

**Per-dataset bar charts.** The following bar charts compare **PACIFIER** with all baselines on each dataset under the cost-weighted setting. Lower values indicate better trajectory-aware performance (area-under-curve / accumulated metric).

**Discussion.** We next analyze the real-world results under the cost-aware setting. Unlike the main real-world benchmark in Sec. 5.5, here we report only per-dataset bar comparisons, so the discussion focuses on cross-dataset performance patterns visible from these bars, together with subset-based summary statistics when **BOMP** is only partially available. A particularly important addition in this setting is the **cost** baseline, which constructs the intervention sequence simply by sorting nodes in ascending order of intervention cost. Because this rule ignores both opinion information and graph structure, its performance directly reveals how much of the task can already be solved by pure low-cost preference alone.

**Evaluation protocol note.** As in the other real-world experiments, all cost-aware results are evaluated on the same 15 polarized topic graphs. However, **BOMP** remains only partially available due to its computational cost on larger instances. For both cost-MI and cost-ME, BOMP is available on 10 of the 15 datasets. Therefore, whenever BOMP is discussed, its averages should be interpreted only on the corresponding BOMP-comparable subset, rather than as directly comparable to full-coverage averages of methods such as PACIFIER. Accordingly, in the task-specific discussion below, we distinguish (i) comparisons on the BOMP-comparable subset and (ii) comparisons on the full dataset collection excluding BOMP from the strongest-baseline reference.

**Cost-MI.** The cost-MI results reveal a qualitatively different pattern from the standard MI setting. Once intervention cost is introduced, the newly added **cost** baseline becomes immediately dominant among the non-PACIFIER methods, and in fact emerges as the strongest baseline overall on average. On the 10-dataset BOMP-comparable subset, **cost** achieves the best average AUC (0.158), slightly ahead of **PACIFIER-Greedy** (0.158) and more clearly ahead of **PACIFIER-RL** (0.166), while **BOMP** drops far behind (0.257). Thus, unlike the original MI benchmark where **BOMP**

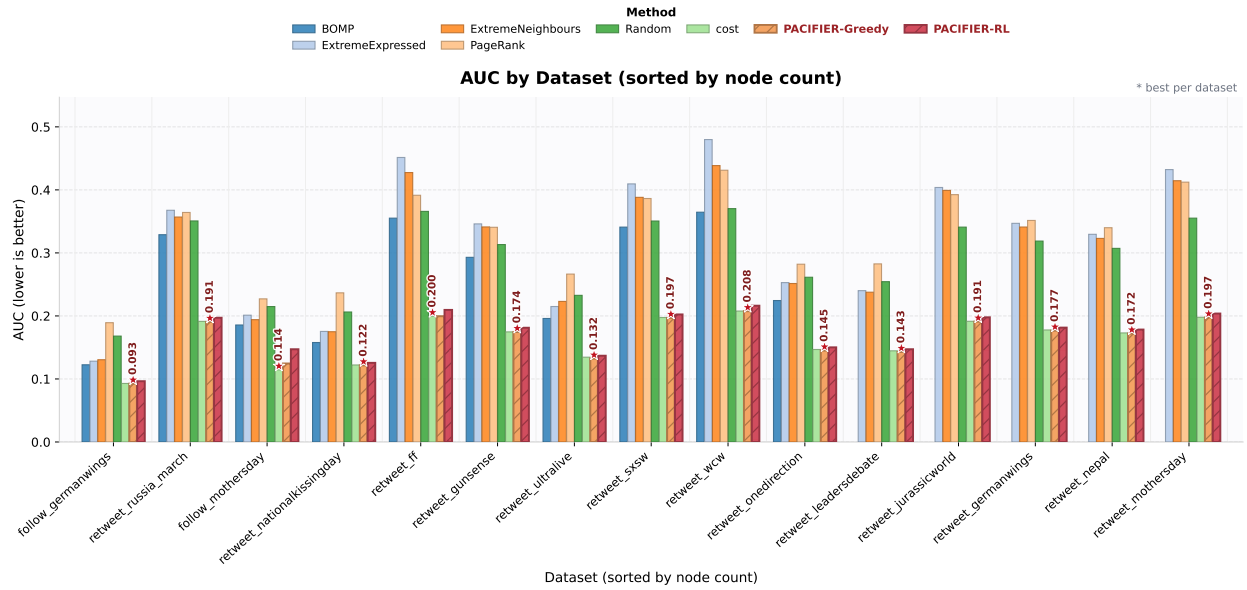


Figure 12: Real datasets (cost-MI): per-dataset bar comparison (lower is better).

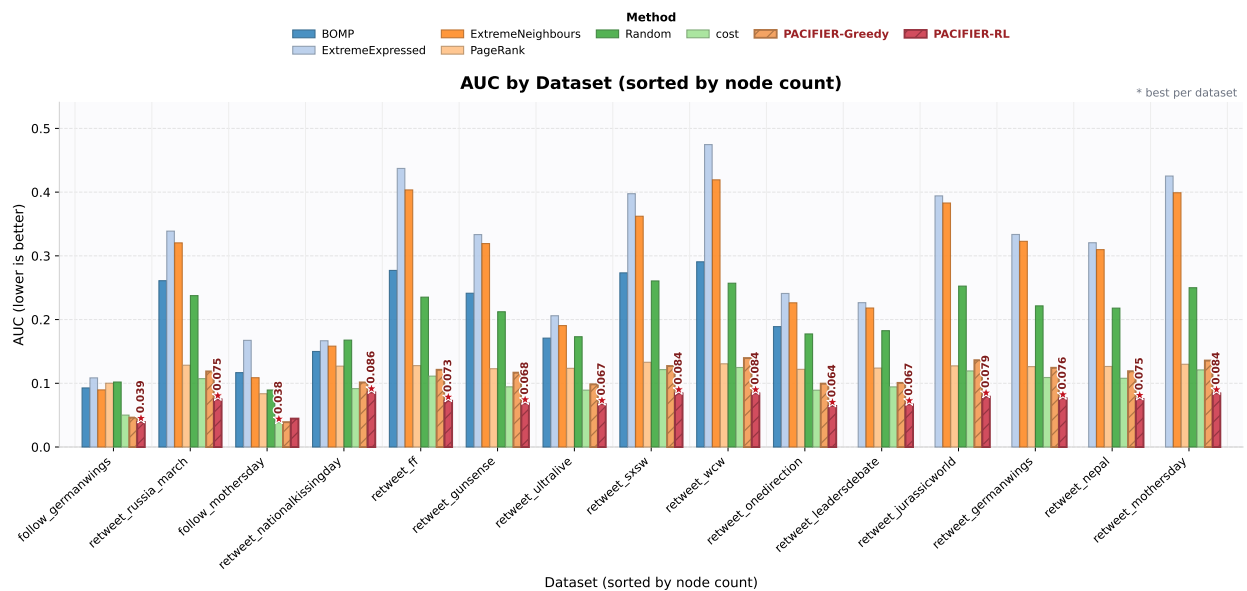


Figure 13: Real datasets (cost-ME): per-dataset bar comparison (lower is better).

was the strongest method whenever available, under cost-aware internal-opinion moderation the primary competitive pressure no longer comes from the analytical solver, but from the extremely simple strategy of always choosing the cheapest nodes first.

This is a meaningful result in itself. It shows that in cost-MI, intervention cost is not a secondary nuisance variable but a central part of the optimization landscape. A baseline that ignores opinions and topology entirely, and uses only the cost weights, is already very hard to beat. This suggests that once the objective is cost-weighted, the benefit of sophisticated influence reasoning can be substantially compressed, because a large part of the achievable advantage is already captured by preferring low-cost interventions.

Against this strong baseline, the two PACIFIER variants behave quite differently. **PACIFIER-RL** does not outperform the strongest non-PACIFIER baseline on any dataset: its win rate is 0/10 on the BOMP-comparable subset and 0/15 on the full dataset collection excluding BOMP. Its mean improvement relative to the strongest non-PACIFIER baseline is

negative in both views. By contrast, **PACIFIER-Greedy** is much more competitive. Although its average improvement is extremely small in magnitude, it stays essentially tied with **cost** overall and in fact wins on most datasets: 8/10 on the BOMP-comparable subset and 13/15 on the full dataset collection excluding BOMP. Its average AUC on the full dataset collection (0.164312) is also marginally lower than that of **cost** (0.164414).

This distinction between the two PACIFIER variants is highly informative. It suggests that cost-MI is a regime where strong performance depends less on long-horizon planning and more on making highly accurate local trade-offs between immediate polarization reduction and intervention cost. In such a regime, a myopic learned ranking policy is naturally better matched to the task than a more heavily bootstrapped RL objective. Indeed, **PACIFIER-Greedy** can be interpreted as learning a refined cost-aware priority rule that stays very close to the strong **cost** heuristic while still extracting a small but consistent extra gain on most datasets. **PACIFIER-RL**, on the other hand, appears to overemphasize longer-horizon structure that is less useful in this particular cost-aware internal-opinion setting.

Another notable consequence is that the relative ordering of classical baselines changes substantially once costs are introduced. In the original MI benchmark, **BOMP** was the clear strongest reference whenever available. Here, however, **BOMP** is no longer competitive, and the simple **cost** ordering dominates not only **Random** and the opinion-based heuristics, but also the analytical baseline itself. This indicates that the cost-aware extension is not a minor perturbation of the original problem, but rather a substantially different regime in which the dominant signal shifts from pure influence structure to cost-effectiveness.

Taken together, the cost-MI results support a nuanced conclusion. They do not show a broad PACIFIER victory in the same sense as the main ME experiments. Instead, they show that the newly introduced **cost** baseline is already extremely strong, that **PACIFIER-Greedy** is able to match and slightly exceed it overall, and that long-horizon RL is not always the best bias when the task is dominated by immediate cost-effectiveness. This makes cost-MI an important counterpoint in the paper: it highlights that PACIFIER is not uniformly superior in every extended setting, and that the relative merits of greedy versus RL policies depend strongly on the structure of the intervention objective.

**Cost-ME.** The picture changes sharply in cost-ME. Here, the **cost** baseline again emerges as the strongest non-PACIFIER competitor, but unlike in cost-MI, it is now decisively surpassed by **PACIFIER-RL**. On the 10-dataset BOMP-comparable subset, **PACIFIER-RL** achieves the best average AUC (0.0685), well ahead of **cost** (0.0917), **PACIFIER-Greedy** (0.1007), and all classical baselines. Even on the full 15-dataset comparison excluding BOMP, **PACIFIER-RL** remains clearly best with an average AUC of 0.0711, compared with 0.0979 for **cost**. Its win rate reaches 9/10 on the BOMP-comparable subset and 14/15 on the full dataset collection, with mean improvements of 21.97% and 24.88%, respectively, over the strongest non-PACIFIER baseline.

This is perhaps the clearest evidence in the cost-aware experiments that PACIFIER-RL learns something substantially beyond simple cost preference. If cost alone were the dominant signal in cost-ME, then the **cost** baseline would be difficult to beat, as it is in cost-MI. Instead, **PACIFIER-RL** achieves large and highly consistent improvements over that baseline, which implies that effective cost-aware expressed-opinion moderation requires jointly reasoning about intervention cost, opinion state, and graph structure over the entire sequence. In other words, in cost-ME it is not enough to intervene cheaply; one must intervene cheaply *and* in the right places and order.

The behavior of **PACIFIER-Greedy** further reinforces this interpretation. Unlike in cost-MI, where the greedy variant is nearly tied with **cost**, in cost-ME it performs substantially worse. It wins on only 1/10 datasets on the BOMP-comparable subset and 1/15 on the full dataset collection excluding BOMP, with clearly negative mean improvements relative to the strongest non-PACIFIER baseline. Thus, in cost-ME, a myopic ranking rule is not sufficient. The fact that **PACIFIER-RL** succeeds while **PACIFIER-Greedy** does not indicates that longer-horizon sequential dependencies are genuinely important in this task.

This RL-versus-Greedy contrast also helps clarify the task difference between cost-MI and cost-ME. In cost-MI, the main challenge appears to be selecting cheap interventions with strong immediate payoff, which favors simple cost ordering and myopic learned refinement. In cost-ME, by contrast, intervening on one node changes the future expressed-opinion landscape in a way that makes later decisions strongly path-dependent. That is exactly the type of setting where bootstrapped long-horizon value learning should help, and the strong empirical advantage of **PACIFIER-RL** is fully consistent with that intuition.

It is also notable that the classical opinion-aware baselines remain very weak in this regime. Both **ExtremeExpressed** and **ExtremeNeighbours** perform far worse than **cost**, **PACIFIER-Greedy**, and especially **PACIFIER-RL**. This indicates that once explicit cost constraints are imposed, naive extremeness-based heuristics can become severely misaligned with the true optimization objective. The challenge is no longer simply to find influential or extreme nodes, but to find interventions with the best cumulative cost-adjusted effect over the trajectory.

Overall, the cost-ME results provide a strong positive result for PACIFIER. They show that the framework does not merely remain usable after adding cost constraints, but that its RL variant can substantially outperform both classical baselines and the newly introduced cost-only heuristic. This makes cost-ME one of the strongest demonstrations in the paper of the value of learned sequential planning under more realistic intervention constraints.

**Overall picture in the cost-aware setting.** Taken together, the cost-aware results reveal a clear task-dependent pattern. For cost-MI, the simple **cost** baseline is already extremely strong, showing that much of the objective can be captured by pure low-cost preference. In this regime, **PACIFIER-Greedy** is the better PACIFIER variant: it essentially matches and slightly exceeds the cost-only rule overall, whereas **PACIFIER-RL** does not obtain an advantage. For cost-ME, by contrast, pure cost preference is no longer enough. Although the **cost** baseline remains the strongest non-PACIFIER competitor, **PACIFIER-RL** decisively outperforms it across almost all datasets, while **PACIFIER-Greedy** falls behind. This contrast strongly supports the broader claim of the paper: the value of PACIFIER depends on the degree to which the intervention task requires genuine sequential planning. When the problem is dominated by immediate cost-effectiveness, a greedy policy can be sufficient or even preferable; when future interaction effects matter, as in cost-ME, long-horizon RL becomes clearly advantageous.

**Summary of real-world results.** Taken together, the real-world results reveal a clear and task-dependent overall pattern across both the canonical and extended settings. Throughout all these experiments, PACIFIER transfers non-trivially from synthetic training graphs to heterogeneous real-world networks, indicating that it captures meaningful intervention structure rather than merely overfitting to synthetic instances. At the same time, the strength and form of this transfer vary substantially across regimes, and these differences are themselves highly informative about when learning—and especially long-horizon RL—is most valuable.

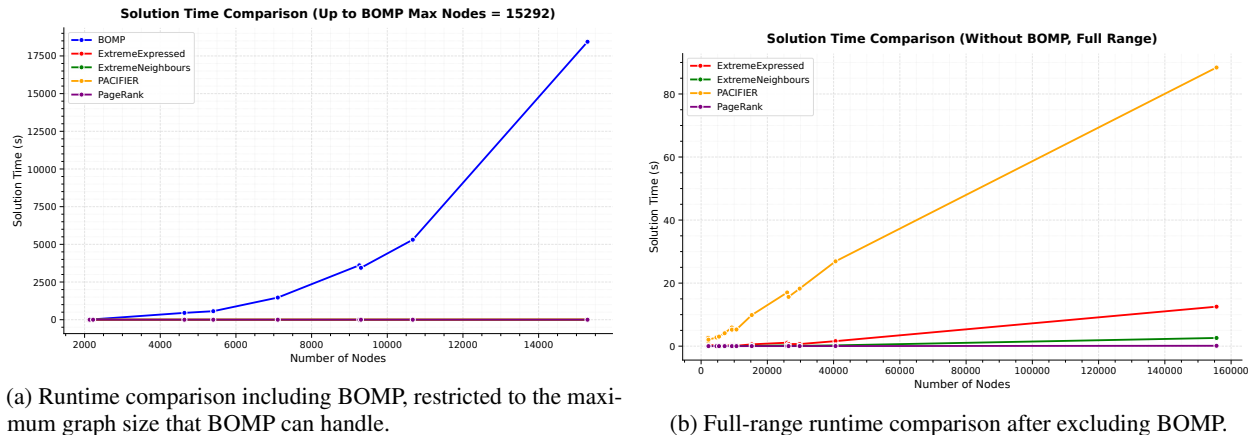
For the analytically structured MI family, including both the standard and continuous settings, the strongest analytical baseline remains difficult to surpass whenever it is computationally feasible. In particular, BOMP continues to dominate in standard MI and continuous-MI, showing that when the problem remains closely aligned with linear influence structure, analytical reasoning still provides a very strong inductive bias. Nevertheless, PACIFIER already becomes highly competitive once the comparison shifts to scalable non-PACIFIER baselines, and **PACIFIER-RL** consistently emerges as the strongest learned or non-analytical alternative in these regimes. This indicates that even where learning does not fully replace analytical structure, it still captures useful intervention patterns that transfer meaningfully to real graphs.

A much stronger picture emerges for the ME family. In standard ME and continuous-ME, both PACIFIER variants consistently outperform all non-PACIFIER baselines across the real-world benchmark, demonstrating robust transfer of the learned intervention strategy beyond the synthetic training distribution. However, the cost-aware setting reveals a sharper separation between the two learned variants. In **cost-ME**, **PACIFIER-RL** substantially outperforms not only all classical baselines but also the strong cost-only baseline, whereas **PACIFIER-Greedy** falls clearly behind. This is one of the clearest signs in the paper that long-horizon reasoning matters: once intervention quality depends on how current budget-aware choices shape future expressed-opinion trajectories, RL gains a decisive advantage over myopic ranking.

The contrast with **cost-MI** is equally revealing. There, the newly introduced **cost** baseline becomes extremely strong, and **PACIFIER-Greedy** remains essentially tied with it, even slightly ahead overall, while **PACIFIER-RL** does not obtain an advantage. This suggests that cost-MI is dominated more by immediate cost-effectiveness than by deep sequential dependencies, and therefore does not reward long-horizon planning in the same way as cost-ME. Rather than weakening the overall argument, this contrast strengthens it: the experiments show that RL is most beneficial precisely in those settings where future interaction effects are genuinely important, not simply everywhere by default.

Finally, *node\_removal* provides the strongest evidence that explicit sequential planning is essential. Here, **PACIFIER-RL** consistently and substantially outperforms both classical baselines and **PACIFIER-Greedy**, indicating that effective intervention depends critically on modeling the long-term structural consequences of each action. Among all the tasks considered, this is the regime where the distinction between myopic ranking and true long-horizon planning becomes most pronounced, and where the value of the RL formulation is most clearly exposed.

Overall, the real-world results show that PACIFIER achieves meaningful transfer across a broad spectrum of moderation regimes, while also revealing a sharp and interpretable pattern in the relative value of its two variants. **PACIFIER-RL** is not merely competitive in general; it is especially powerful in settings where analytical structure is weaker or where genuinely sequential, path-dependent planning is required, such as cost-ME and *node\_removal*. By contrast, when the task is dominated by immediate local trade-offs, as in cost-MI, the gap between RL and myopic ranking narrows substantially. This regime-dependent picture is itself a central result of the paper: it shows not only that PACIFIER



(a) Runtime comparison including BOMP, restricted to the maximum graph size that BOMP can handle.

(b) Full-range runtime comparison after excluding BOMP.

Figure 14: Runtime comparison on real-world datasets under the standard setting. Left: all methods are compared within the node-size range where BOMP remains executable. Right: after removing BOMP, the full-range scaling behavior of the remaining methods is shown. Overall, BOMP exhibits a much steeper growth trend than the other approaches, whereas PACIFIER remains scalable on large graphs.

transfers to real networks, but also *when* and *why* long-horizon graph reinforcement learning provides its greatest advantage.

## 5.7 Runtime in the Standard Setting

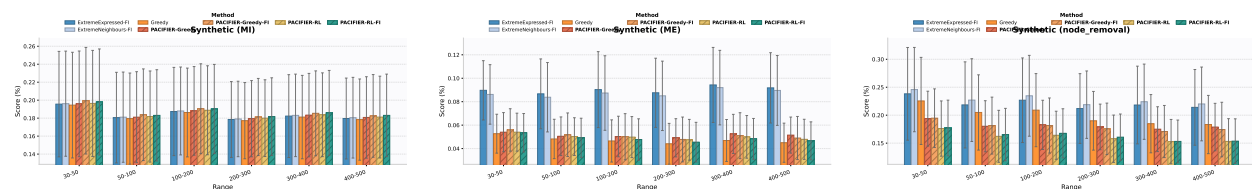
We further compare the empirical runtime of all methods on the real-world datasets under the standard setting. Figure 14 presents two complementary views: (i) a comparison restricted to the node range covered by BOMP, and (ii) a full-range comparison after excluding BOMP. Together, these results illustrate the substantial scalability gap between BOMP and the remaining methods.

**Discussion.** The runtime results reveal a clear scalability distinction between BOMP and the remaining methods. According to the complexity analysis of Matakos et al., **BOMP** has time complexity  $O(kn^2)$ , where  $n$  is the number of nodes and  $k$  is the intervention budget. Its high computational cost mainly comes from dense matrix-based candidate scoring built on the influence matrix  $Q = (L + I)^{-1}$ . In each iteration, BOMP repeatedly evaluates candidate nodes using dense influence information, which leads to a quadratic dependence on graph size and makes the method increasingly expensive on large graphs. By contrast, the lighter baselines used here are computationally cheaper: **ExtremeExpressed** has complexity  $O(kn)$  in the MI setting, **ExtremeNeighbours** has complexity  $O(k(n + m))$ , and **PageRank** has complexity  $O((m + n)I + n \log n)$ , where  $m$  is the number of edges and  $I$  is the number of power-iteration steps.

This complexity gap is also clearly reflected in Fig. 14a. Within the node range where BOMP remains executable, its runtime grows dramatically with graph size and reaches about  $1.8 \times 10^4$  seconds at the largest supported graph. In contrast, the other methods remain close to the bottom of the plot throughout the same range, and even the slowest among them is still lower by several orders of magnitude. This visual gap is consistent with the theoretical distinction between BOMP’s quadratic dependence on  $n$  and the much lighter sparse-graph-oriented cost of the remaining methods.

For **PACIFIER**, the deployment-time complexity can be characterized directly from its feed-forward inference pipeline. In the application phase, the encoder performs a constant number  $K$  of GraphSAGE-style message-passing rounds, which costs  $O(K(n + m))$  on a sparse graph. The decoder then scores all candidate nodes in parallel, contributing an additional  $O(n)$  term. If the final action is obtained through ranking or batch selection over all node scores, this adds an  $O(n \log n)$  step. Therefore, the overall application-time complexity of PACIFIER is  $O(K(n + m) + n \log n)$ , which reduces to approximately  $O(n + m + n \log n)$  when  $K$  is treated as a small constant. Strictly speaking, this is not pure linear complexity in the formal sense, but it is near-linear in sparse graphs and is far milder than the quadratic  $O(kn^2)$  behavior of BOMP.

This near-linear scaling trend is consistent with Fig. 14b. After excluding BOMP, all remaining methods show much gentler growth across the full graph range. Among them, PACIFIER is slower than the lightest baselines, especially on the largest graph where its runtime is around 89 seconds, while the next slowest method remains around 13 seconds. However, despite this moderate overhead, PACIFIER follows the same overall near-linear sparse-graph scaling regime



(a) MI on synthetic graphs under full-information comparison.

(b) ME on synthetic graphs under full-information comparison.

(c) NODE-REMOVAL on synthetic graphs under full-information comparison.

Figure 15: Synthetic full-information comparison across three representative settings: MI, ME, and NODE-REMOVAL. Methods with the suffix **-FI** are allowed to access recomputed intermediate settled-opinion states during sequential selection, while methods without this suffix remain in the standard one-shot regime unless otherwise noted. The **Greedy** baseline is an oracle-style full-information replanning method that performs exhaustive one-step trial, rollback, and reselection at each decision step. Lower ANP indicates better trajectory-level polarization moderation performance.

as the other non-BOMP methods, rather than exhibiting the steep superlinear explosion observed for BOMP. This additional cost is acceptable in practice given its stronger moderation performance in the more challenging settings. Importantly, PACIFIER does not rely on dense influence-matrix operations for each candidate node during deployment. Instead, it uses a feed-forward inference pipeline in which the encoder and decoder directly produce action scores from graph representations. These differences explain why its empirical runtime grows much more gently and remains practical even on the largest real-world graphs in our benchmark.

## 5.8 Synthetic Benchmark: Full-Information Comparison

To further examine the role of intermediate steady-state information, we conduct an additional comparison on *synthetic* graphs under a *full-information* (FI) setting. Unlike the standard one-shot planning regime adopted throughout the main paper, the FI setting allows an algorithm to access the recomputed settled-opinion state after each partial intervention step. In other words, FI methods are allowed to use intermediate steady-state expressed opinions during sequential selection, and therefore do not satisfy the one-shot planning constraint defined in Sec. 3.4.

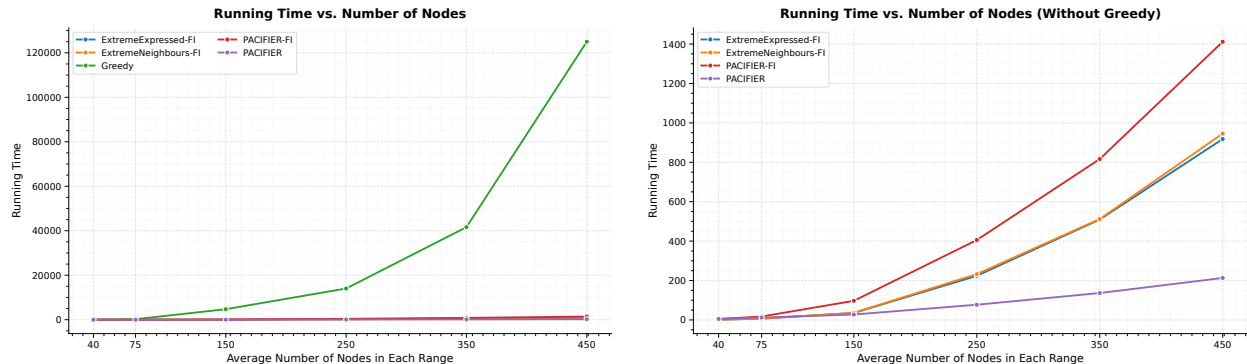
The purpose of this experiment is not to propose a new deployment setting, but to clarify how much performance can be gained when intermediate settled-opinion information is explicitly exposed to the planner. This comparison helps distinguish the contribution of learned planning under the practical one-shot regime from the contribution of additional oracle-like state information.

The compared methods follow the naming convention introduced in Sec. 5.3: methods with the suffix **-FI** are their full-information variants, while methods without this suffix remain in the standard one-shot regime. Accordingly, this benchmark includes the FI variants of heuristic and learned methods, together with a strong oracle-style greedy replanning baseline. Concretely, we compare **ExtremeExpressed-FI**, **ExtremeNeighbours-FI**, **PACIFIER-RL**, **PACIFIER-Greedy**, **PACIFIER-RL-FI**, **PACIFIER-Greedy-FI**, and **Greedy**. Among these methods, all entries marked with the suffix **-FI** as well as **Greedy** explicitly use intermediate settled-opinion information, whereas **PACIFIER-RL** and **PACIFIER-Greedy** do not. Therefore, this experiment directly measures the gap between one-shot planning and sequential replanning with full access to recomputed intermediate steady-state information.

We evaluate these methods on synthetic graphs under three representative settings: MI, ME, and topology-altering NODE-REMOVAL. The reported metric is the same trajectory-level accumulated normalized polarization (ANP) used in the main experiments, where lower values indicate better overall intervention quality.

**Discussion.** The performance comparison in Fig. 15 leads to three main observations. First, exposing intermediate settled-opinion states is indeed helpful, but it does not fundamentally change the overall picture. Across MI, ME, and NODE-REMOVAL, methods with access to full information generally benefit from the additional feedback, yet the gains are typically incremental rather than transformative. In particular, the PACIFIER family remains highly competitive even when compared against baselines that are allowed to replan using recomputed intermediate steady states.

Second, the relatively small gap between the standard one-shot PACIFIER variants and their FI counterparts suggests that the main source of performance does not come merely from access to oracle-like intermediate information. Rather, it comes from the quality of the learned intervention policy itself. This point is especially important because **PACIFIER-RL** and **PACIFIER-Greedy** operate under a strictly weaker information regime than all **-FI** methods and the exhaustive **Greedy** baseline. That they still remain among the strongest methods indicates that effective long-horizon planning can recover most of the obtainable benefit without requiring sequential recomputation of the settled state after every step.



(a) Runtime comparison of all methods under the full-information setting. (b) Runtime comparison under the full-information setting after removing Greedy.

Figure 16: Runtime comparison on synthetic graphs under the full-information setting. Left: all methods are included. Right: the **Greedy** baseline is removed to make the differences among the remaining methods easier to observe. Overall, FI-based sequential replanning introduces substantial extra computational cost, while the standard PACIFIER remains markedly more efficient than the FI baselines.

Third, the three synthetic settings also reveal that the value of FI depends on the intervention type. For MI and ME, FI access provides additional adaptivity during sequential selection, but learned planning remains the dominant factor in achieving low ANP. For topology-altering **NODE-REMOVAL**, the problem becomes more challenging because each intervention changes not only the opinion configuration but also the underlying interaction structure. In this setting, purely myopic improvement based on refreshed intermediate states is not sufficient to guarantee the best trajectory-level outcome, which highlights the importance of planning beyond immediate one-step gain.

Overall, the synthetic full-information comparison supports a clear conclusion: intermediate steady-state information is useful, but it is not the primary reason PACIFIER performs well. The proposed learned policies already capture most of the achievable moderation benefit under the practical one-shot regime, while FI-style sequential replanning mainly provides limited additional improvement rather than altering the qualitative conclusion of the study. This strengthens the case for PACIFIER as a practical approach: strong moderation performance can be achieved without assuming access to recomputed intermediate settled-opinion states during deployment.

## 5.9 Runtime in the Full-Information Setting

In practice, intermediate settled-opinion states are typically unavailable during deployment, which is one of the main reasons why our standard setting does not rely on such information. Therefore, the purpose of this runtime comparison is not to characterize practical deployment cost under realistic access assumptions, but to show, in a simulation setting, how much time different FI-style methods require when intermediate converged opinion states are explicitly recomputed and used during sequential selection.

We further compare the empirical runtime of all methods under the full-information (FI) setting. Figure 16 presents two complementary views: (i) a runtime comparison including all methods, and (ii) a comparison after removing the **Greedy** baseline. Together, these results reveal the substantial computational overhead introduced by FI-style sequential replanning.

**Discussion.** The runtime results in Fig. 16 show a clear efficiency gap between the standard PACIFIER and FI-based methods when intermediate converged opinion states are explicitly recomputed in simulation.

From Fig. 16a, the most striking pattern is the explosive growth of **Greedy**. As the average graph size increases from 40 to 450 nodes, its running time rises from nearly negligible values to about  $1.25 \times 10^5$ , far exceeding all other methods. This shows that exhaustive full-information replanning becomes extremely costly once the graph size grows.

After removing **Greedy**, Fig. 16b makes the comparison among the remaining methods much clearer. The overall pattern is highly consistent: methods that rely on FI-style sequential replanning all incur substantially higher runtime, whereas the standard **PACIFIER** remains much faster across the full graph range. At 250 nodes, **PACIFIER** requires only about 75 runtime units, while the FI methods are already around 225–230 for **ExtremeExpressed-FI** and **ExtremeNeighbours-FI**, and above 400 for **PACIFIER-FI**. At 350 nodes, the standard **PACIFIER** is still only about

Table 5: Ablation study under the MI setting with the greedy mechanism on real-world datasets (ANP; lower is better).

ANP	follow_germanwings	follow_mothersday	retweet_wcw	retweet_onedirection	retweet_mothersday	retweet_russia_march	retweet_leadersdebate	%
PACIFIER-Greedy	0.1359	<b>0.2033</b>	0.4101	0.2488	0.4000	0.3562	0.2372	–
PACIFIER-Greedy-without_aux	0.1532 (-12.71%)	0.2134 (-4.99%)	<b>0.3978 (+3.01%)</b>	<b>0.2424 (+2.56%)</b>	<b>0.3943 (+1.42%)</b>	0.3456 (+2.99%)	0.2396 (-1.01%)	<b>-0.62%</b>
PACIFIER-Greedy-without_mask1	<b>0.1330 (+2.15%)</b>	0.2053 (-1.02%)	0.3982 (+2.90%)	0.2456 (+1.28%)	0.4047 (-1.17%)	<b>0.3442 (+3.38%)</b>	<b>0.2362 (+0.39%)</b>	<b>+1.45%</b>
PACIFIER-Greedy-without_mask2	0.2383 (-75.33%)	0.2977 (-46.43%)	0.4704 (-14.70%)	0.3240 (-30.21%)	0.4506 (-12.65%)	0.4264 (-19.70%)	0.3246 (-36.88%)	<b>-29.05%</b>
ANP	retweet_jurassicworld	retweet_germanwings	retweet_nepal	retweet_nationalkissingday	retweet_ff	retweet_gunsense	retweet_ultralive	retweet_sxsw
PACIFIER-Greedy	0.3633	0.3304	0.3200	<b>0.1733</b>	0.3894	0.3162	0.2124	0.3647
PACIFIER-Greedy-without_aux	0.3563 (+1.92%)	0.3285 (+0.58%)	0.3145 (+1.71%)	0.1819 (-4.97%)	0.3757 (+3.50%)	0.3111 (+1.61%)	0.2229 (-4.95%)	<b>0.3642 (+0.13%)</b>
PACIFIER-Greedy-without_mask1	<b>0.3546 (+2.39%)</b>	<b>0.3245 (+1.81%)</b>	<b>0.3111 (+2.76%)</b>	0.1734 (-0.06%)	<b>0.3724 (+4.37%)</b>	<b>0.3078 (+2.67%)</b>	<b>0.2107 (+0.79%)</b>	0.3678 (-0.86%)
PACIFIER-Greedy-without_mask2	0.4260 (-17.24%)	0.4002 (-21.13%)	0.3825 (-19.55%)	0.2448 (-41.26%)	0.4542 (-16.64%)	0.3904 (-23.47%)	0.3001 (-41.29%)	0.4351 (-19.31%)

Table 6: Ablation study under the MI setting with RL on real-world datasets (ANP; lower is better).

ANP	follow_germanwings	follow_mothersday	retweet_wcw	retweet_onedirection	retweet_mothersday	retweet_russia_march	retweet_leadersdebate	%
PACIFIER-RL	<b>0.1328</b>	<b>0.2002</b>	0.4087	<b>0.2360</b>	<b>0.3980</b>	<b>0.3436</b>	<b>0.2285</b>	–
PACIFIER-RL-without_aux	0.1573 (-18.43%)	0.2243 (-12.01%)	<b>0.4010 (+1.89%)</b>	0.2574 (-9.06%)	0.4041 (-1.53%)	0.3545 (-3.16%)	0.2551 (-11.64%)	<b>-5.38%</b>
PACIFIER-RL-without_mask1	0.1341 (-0.98%)	0.2124 (-6.09%)	0.4253 (-4.06%)	0.2446 (-3.64%)	0.4036 (-1.40%)	0.3570 (-3.90%)	0.2354 (-3.02%)	<b>-3.30%</b>
PACIFIER-RL-without_mask2	0.1572 (-18.34%)	0.2077 (-3.75%)	0.4071 (+0.39%)	0.2475 (-4.87%)	0.4027 (-1.18%)	0.3601 (-4.81%)	0.2471 (-8.14%)	<b>-4.36%</b>
ANP	retweet_jurassicworld	retweet_germanwings	retweet_nepal	retweet_nationalkissingday	retweet_ff	retweet_gunsense	retweet_ultralive	retweet_sxsw
PACIFIER-RL	<b>0.3612</b>	<b>0.3281</b>	<b>0.3033</b>	0.1739	0.3827	<b>0.3067</b>	<b>0.2064</b>	<b>0.3653</b>
PACIFIER-RL-without_aux	0.3631 (-0.53%)	0.3423 (-4.33%)	0.3198 (-5.44%)	0.1760 (-1.21%)	<b>0.3769 (+1.52%)</b>	0.3204 (-4.47%)	0.2315 (-12.16%)	0.3658 (-0.14%)
PACIFIER-RL-without_mask1	0.3689 (-2.13%)	0.3292 (-0.34%)	0.3139 (-3.49%)	0.1876 (-7.88%)	0.4055 (-5.96%)	0.3095 (-0.91%)	0.2127 (-3.05%)	0.3749 (-2.63%)
PACIFIER-RL-without_mask2	0.3663 (-1.41%)	0.3397 (-3.53%)	0.3166 (-4.39%)	<b>0.1732 (+0.40%)</b>	0.3819 (+0.21%)	0.3202 (-4.40%)	0.2266 (-9.79%)	0.3720 (-1.83%)

135, whereas the FI methods have increased to roughly 500 and above. At 450 nodes, **PACIFIER** remains around 210, while the three FI methods all stay much higher, ending around 920, 950, and 1410, respectively.

These results indicate that once intermediate converged opinion states are inserted into the decision loop, the runtime overhead rises sharply, regardless of the specific FI method used. In this sense, **PACIFIER-FI**, like the other FI algorithms, also bears the substantial computational burden brought by sequential full-information replanning. By contrast, the standard one-shot **PACIFIER** maintains a far more favorable runtime profile throughout all graph ranges.

Overall, this comparison supports a clear conclusion: although FI-style replanning can provide additional intermediate information in simulation, it comes with a pronounced computational cost. The standard one-shot **PACIFIER**, while maintaining strong performance, also demonstrates excellent computational efficiency. This advantage becomes increasingly clear as the graph size grows, further highlighting the practical value of the one-shot PACIFIER design.

## 5.10 Ablation Study

To validate the necessity of the two key representation components in PACIFIER, namely the *polarization-aware auxiliary features* and the *temporal-aware node marking*, we conduct a comprehensive ablation study on the real-world benchmark under both the MI and ME settings, each with two decision mechanisms: the greedy strategy and reinforcement learning. For each mechanism, we compare the full PACIFIER model against three ablated variants: removing the polarization-aware auxiliary features (*without\_aux*), removing the first temporal marking component (*without\_mask1*), and removing the second temporal marking component (*without\_mask2*). The reported metric is ANP, where lower values indicate better trajectory-level moderation performance. For each dataset column, the best (lowest) score is highlighted in bold. The last column reports the average relative improvement of each ablated variant with respect to the corresponding full model.

**Discussion.** Tables 5–8 show that the two proposed representation components contribute differently across tasks and decision mechanisms, although temporal-aware marking remains important throughout.

Under the greedy MI mechanism, removing the auxiliary polarization-aware features causes only a very small average degradation overall (−0.62%), and *without\_aux* even slightly improves over the full model on several datasets, including *retweet\_wcw*, *retweet\_onedirection*, *retweet\_mothersday*, *retweet\_russia\_march*, and several datasets in the second half of the table. This suggests that, in the myopic MI regime, the auxiliary graph-level polarization signals provide limited and somewhat unstable benefit. Interestingly, removing *mask1* yields a small average gain of +1.45%, indicating that this marking variant is not consistently necessary for greedy MI and may be partially redundant in this setting. In contrast, removing *mask2* leads to a dramatic average degradation of 29.05%, showing that the second temporal marking component is the dominant contributor under greedy MI. Overall, these results suggest that, in the greedy MI regime, explicit intervention-history encoding remains important, but its benefit is concentrated mainly in *mask2* rather than being evenly distributed across both marking components.

Table 7: Ablation study under the ME setting with the greedy mechanism on real-world datasets (ANP; lower is better).

ANP	follow_germanwings	follow_mothersday	retweet_wcw	retweet_onedirection	retweet_mothersday	retweet_russia_march	retweet_leadersdebate	%
PACIFIER-Greedy	0.0619	0.0559	<b>0.1187</b>	0.0864	<b>0.1159</b>	<b>0.1010</b>	<b>0.0888</b>	-
PACIFIER-Greedy-without_aux	<b>0.0597 (+3.48%)</b>	<b>0.0552 (+1.24%)</b>	0.1213 (-2.17%)	<b>0.0861 (+0.36%)</b>	0.1188 (-2.51%)	0.1026 (-1.52%)	0.0902 (-1.63%)	<b>-0.93%</b>
PACIFIER-Greedy-without_mask1	0.0663 (-7.05%)	0.0647 (-15.76%)	0.1237 (-4.17%)	0.0954 (-10.48%)	0.1188 (-2.51%)	0.1112 (-10.04%)	0.0972 (-9.53%)	<b>-8.19%</b>
PACIFIER-Greedy-without_mask2	0.1117 (-80.49%)	0.1334 (-138.88%)	0.1321 (-11.27%)	0.1249 (-44.60%)	0.1302 (-12.32%)	0.1310 (-29.70%)	0.1274 (-43.47%)	<b>-36.15%</b>
ANP	retweet_jurassicworld	retweet_germanwings	retweet_nepal	retweet_nationalkissingday	retweet_ff	retweet_gunsense	retweet_ultralive	retweet_sxsw
PACIFIER-Greedy	<b>0.1089</b>	<b>0.1028</b>	<b>0.1021</b>	0.1239	<b>0.1004</b>	<b>0.0938</b>	<b>0.0899</b>	<b>0.1172</b>
PACIFIER-Greedy-without_aux	0.1113 (-2.19%)	0.1054 (-2.50%)	0.1033 (-1.13%)	<b>0.1238 (+0.05%)</b>	0.1010 (-0.64%)	0.0959 (-2.18%)	0.0920 (-2.28%)	0.1176 (-0.35%)
PACIFIER-Greedy-without_mask1	0.1170 (-7.47%)	0.1109 (-7.84%)	0.1068 (-4.51%)	0.1259 (-1.61%)	0.1132 (-12.79%)	0.1092 (-16.39%)	0.0983 (-9.29%)	0.1213 (-3.48%)
PACIFIER-Greedy-without_mask2	0.1262 (-15.92%)	0.1269 (-23.49%)	0.1276 (-24.88%)	0.1270 (-2.54%)	0.1301 (-29.60%)	0.1229 (-30.99%)	0.1243 (-38.21%)	0.1358 (-15.85%)

Table 8: Ablation study under the ME setting with RL on real-world datasets (ANP; lower is better).

ANP	follow_germanwings	follow_mothersday	retweet_wcw	retweet_onedirection	retweet_mothersday	retweet_russia_march	retweet_leadersdebate	%
PACIFIER-RL	0.0611	<b>0.0573</b>	<b>0.1187</b>	<b>0.0874</b>	<b>0.1163</b>	<b>0.1009</b>	<b>0.0909</b>	-
PACIFIER-RL-without_aux	<b>0.0594 (+2.75%)</b>	0.0882 (-53.86%)	0.1256 (-5.80%)	0.1088 (-24.47%)	0.1224 (-5.31%)	0.1195 (-18.51%)	0.1044 (-14.87%)	<b>-13.85%</b>
PACIFIER-RL-without_mask1	0.0868 (-41.95%)	0.1015 (-77.03%)	0.1257 (-5.87%)	0.1137 (-30.06%)	0.1250 (-7.49%)	0.1196 (-18.56%)	0.1144 (-25.89%)	<b>-21.83%</b>
PACIFIER-RL-without_mask2	0.1132 (-85.16%)	0.1233 (-115.13%)	0.1312 (-10.53%)	0.1110 (-26.89%)	0.1281 (-10.21%)	0.1227 (-21.68%)	0.1218 (-33.97%)	<b>-28.68%</b>
ANP	retweet_jurassicworld	retweet_germanwings	retweet_nepal	retweet_nationalkissingday	retweet_ff	retweet_gunsense	retweet_ultralive	retweet_sxsw
PACIFIER-RL	<b>0.1101</b>	<b>0.1026</b>	<b>0.1029</b>	<b>0.1231</b>	<b>0.1036</b>	<b>0.0951</b>	<b>0.0917</b>	<b>0.1166</b>
PACIFIER-RL-without_aux	0.1226 (-11.40%)	0.1166 (-13.69%)	0.1159 (-12.56%)	0.1242 (-0.88%)	0.1149 (-11.00%)	0.1082 (-13.77%)	0.1088 (-18.70%)	0.1232 (-5.70%)
PACIFIER-RL-without_mask1	0.1236 (-12.26%)	0.1220 (-18.88%)	0.1192 (-15.80%)	0.1271 (-3.25%)	0.1179 (-13.85%)	0.1187 (-24.78%)	0.1135 (-23.79%)	0.1258 (-7.97%)
PACIFIER-RL-without_mask2	0.1219 (-10.74%)	0.1210 (-17.91%)	0.1197 (-16.32%)	0.1271 (-3.21%)	0.1179 (-13.81%)	0.1185 (-24.66%)	0.1149 (-25.35%)	0.1336 (-14.60%)

Under the RL-based MI mechanism, the same overall pattern remains but becomes milder and more stable. Removing auxiliary features degrades performance by 5.38% on average, while removing mask1 and mask2 leads to average degradations of 3.30% and 4.36%, respectively. The full PACIFIER-RL model achieves the best ANP on most datasets, although `without_aux` slightly improves over the full model on `retweet_wcw` and `retweet_ff`, and `without_mask2` slightly improves on `retweet_nationalkissingday`. This indicates that, under RL for MI, both auxiliary polarization-aware features and temporal-aware marking are helpful, but the overall sensitivity of performance to these components is clearly weaker than in ME. This is consistent with MI being a more analytically structured and comparatively easier setting.

Under the greedy ME mechanism, removing the auxiliary polarization-aware features causes only marginal and inconsistent changes, with an average degradation of 0.93%. In fact, `without_aux` even achieves slightly better ANP on several datasets, such as `follow_germanwings`, `follow_mothersday`, `retweet_onedirection`, and `retweet_nationalkissingday`. This suggests that, for greedy decision making under ME, auxiliary graph-level polarization signals are not consistently critical and their contribution is relatively dataset-dependent. In contrast, temporal-aware node marking plays a much more important role for the greedy ME mechanism. Removing mask1 leads to an average degradation of 8.19%, while removing mask2 causes a substantially larger drop of 36.15%. The especially severe deterioration of `without_mask2` indicates that explicit intervention-history encoding is essential when the greedy policy must distinguish states that are structurally similar but arise from different moderation trajectories.

Under the RL-based ME mechanism, the contribution of both components becomes more substantial. Removing auxiliary features degrades performance by 13.85% on average, while removing the two temporal marking variants results in even larger drops of 21.83% and 28.68%, respectively. Moreover, the full PACIFIER-RL model achieves the best ANP on 14 out of 15 datasets, with only `follow_germanwings` showing a slight improvement for `without_aux`. This indicates that, under RL, both auxiliary polarization-aware features and temporal-aware marking contribute more consistently to policy quality, while temporal-aware marking remains the more critical factor.

Overall, the ablation results suggest that the two representation mechanisms are complementary, but their relative importance depends on both the moderation setting and the decision mechanism. For the greedy variants, auxiliary features provide limited and unstable gains, whereas temporal-aware marking—especially `mask2`—is the dominant factor. For the RL variants, both components are more consistently beneficial, with the effect being particularly strong under ME. These findings support keeping both components in the full PACIFIER framework, while also highlighting that explicit temporal-aware state encoding is the key factor for robust performance across sequential polarization-moderation settings.

## 6 Conclusion

We proposed **PACIFIER**, to our knowledge the first unified graph-learning framework, and in particular the first unified graph reinforcement learning framework, for opinion polarization moderation. In contrast to prior work in this area, which is largely dominated by analytical and model-specific optimization under the Friedkin–Johnsen (FJ) model,

PACIFIER reformulates the canonical MODERATEINTERNAL (MI) and MODERATEEXPRESSED (ME) problems as graph-based sequential decision-making tasks under a practical one-shot planning regime.

To support effective learning in topology-preserving moderation, we introduced two key representation mechanisms: temporal-aware node marking, which makes intervention history explicit and resolves history-induced state aliasing, and polarization-aware auxiliary global features, which summarize opinion–structure interaction patterns without requiring repeated steady-state recomputation. These components enable a shared encode–decode architecture that supports both long-horizon learning (**PACIFIER-RL**) and myopic ranking (**PACIFIER-Greedy**).

Experiments on polarized real-world Twitter follow and retweet graphs reveal a clear regime-dependent picture. In analytically structured MI settings, PACIFIER remains competitive with strong analytical solvers and consistently emerges as the strongest scalable non-analytical alternative. In contrast, in ME, continuous-ME, and cost-ME, PACIFIER shows strong and highly consistent superiority over non-PACIFIER baselines. Most importantly, **PACIFIER-RL** becomes decisively superior when long-horizon planning truly matters, most notably in cost-ME and topology-altering *node\_removal*, where explicit reasoning over future structural consequences is crucial.

These results show that the contribution of PACIFIER is not only algorithmic but also conceptual: it helps identify when polarization moderation remains primarily an analytical optimization problem, and when it should instead be treated as a sequential, path-dependent planning problem. Future work includes extending PACIFIER to multi-camp and multi-topic settings, richer intervention primitives, and a deeper theoretical understanding of when learning can match or surpass analytical methods. Overall, PACIFIER shifts opinion polarization moderation from a domain dominated by model-specific analytical optimization toward a unified graph-learning and graph-reinforcement-learning paradigm.

## Acknowledgments

This was supported in part by.....

## References

- [1] Antonis Matakos, Evimaria Terzi, and Panayiotis Tsaparas. Measuring and moderating opinion polarization in social networks. *Data Mining and Knowledge Discovery*, 31(5):1480–1505, 2017.
- [2] Noah E Friedkin and Eugene C Johnsen. Social influence and opinions. *Journal of Mathematical Sociology*, 15(3-4):193–206, 1990.
- [3] Mohammed Lalou, Mohammed Amin Tahraoui, and Hamamache Kheddouci. The critical node detection problem in networks: a survey. *Computer Science Review*, 28:92–117, 2018.
- [4] Changjun Fan, Li Zeng, Yizhou Sun, and Yang-Yu Liu. Finding key players in complex networks through deep reinforcement learning. *Nature Machine Intelligence*, 2(6):317–324, 2020.
- [5] Kiran Garimella, Gianmarco De Francisci Morales, Aristides Gionis, and Michael Mathioudakis. Reducing controversy by connecting opposing views. In *Proceedings of the Tenth ACM International Conference on Web Search and Data Mining (WSDM '17)*, 2017.
- [6] Yue Wu, Linjiao Li, Qiannan Yu, Jiaxin Gan, and Yi Zhang. Strategies for reducing polarization in social networks. *Chaos, Solitons & Fractals*, 167:113095, 2023.
- [7] Cameron Musco, Christopher Musco, and Charalampos E. Tsourakakis. Minimizing polarization and disagreement in social networks. In *Proceedings of the 2018 World Wide Web Conference (WWW '18)*, 2018.
- [8] Zhiyuan Tu, Jeffrey Chan, Xiuzhen Zhang, and Shazia Sadiq. Adversaries with limited information in the friedkin-johnsen model. In *Proceedings of the 29th ACM SIGKDD Conference on Knowledge Discovery and Data Mining (KDD '23)*, 2023.
- [9] Nicholas Mylonas and Thanassis Spyropoulos. Opinion depolarization in social networks with graph neural networks. *arXiv preprint arXiv:2412.09404*, 2024.
- [10] Ashwin Arulselvan, Clayton W Commander, Lily Elefteriadou, and Panos M Pardalos. Detecting critical nodes in sparse graphs. *Computers & Operations Research*, 36(7):2193–2200, 2009.
- [11] Alfredo Braunstein, Luca Dall’Asta, Guilhem Semerjian, and Lenka Zdeborová. Network dismantling. *Proceedings of the National Academy of Sciences*, 113(44):12368–12373, 2016.
- [12] Kiran Garimella, Gianmarco De Francisci Morales, Aristides Gionis, and Michael Mathioudakis. Quantifying controversy on social media. *ACM Transactions on Social Computing*, 1(1):3:1–3:27, 2018.